UNIVERSITÀ DELLA CALABRIA

DIPARTIMENTO FARMACO-BIOLOGICO

Dottorato di ricerca in
Biochimica cellulare e attività dei farmaci in oncologia
XXV ciclo

Tesi di dottorato
in
Biochimica, biochimica clinica e biologia molecolare
SSD BIO/10 BIO/12 BIO/11

Hypocholesterolemic activity of brutieridin and melitidin enriched fraction from bergamot fruit (*Citrus bergamia*): *in vivo* and *in vitro* studies.

Supervisore
Prof. Vincenza Dolce
Vincenza Dolce

Dottoranda
Emanuela Martello
Emanuela Martello

Coordinatore
Prof. Diego Sisci
Diego Sisci

Anno Accademico 2011-2012

INDEX

INTRODUCTION

1.1 Cholesterol: structure and function

Cholesterol is a 27-carbon, tetracyclic molecule that is amphipathic, with a polar head group (the hydroxyl group at C-3) and a nonpolar hydrocarbon body (the steroid nucleus and the hydrocarbon side chain at C-17), about as long as a 16-carbon fatty acid in its extended form (Fig. 1). Cholesterol plays several structural and metabolic roles that are vital for human biology. It is essential for the structure and function of eukaryotic lipid bilayers [1] and spreads along the entire plasma membrane of the cell, modulating fluidity and concentrating in specialized sphingolipid-rich domains called rafts and caveolae [2]. Cholesterol is also a substrate for steroid hormones and bile salts [3].

However, too much cholesterol can lead to pathological pictures such as atherosclerosis, which is a consequence of the accumulation of cholesterol into the cells of the artery wall where accumulation of cholesterol initiates cardiovascular disease [4] than its biosynthesis is one of the most intensively studied biochemical pathways [5].

Because animal cells obtain cholesterol by a combination of *de novo* synthesis and uptake from the bloodstream, the need for end-product feedback inhibition of this biosynthetic pathway is paramount.

Mammalian cells satisfy most of their cholesterol requirements through receptor-mediated endocytosis of cholesterol-rich plasma lipoproteins. However, when exogenous cholesterol supply is short, or when there is an increased demand for particular nonsterol isoprenoids, cells up-regulate the activity of the mevalonate pathway (Fig. 2), in which sterols and essential mevalonic-derived nonsterol isoprenoids are produced [6].

The mevalonate biosynthetic pathway is a sequel of complex reactions that, besides cholesterol, produces several biomolecules involved in RNA transcription (isopentenyl tRNAs, addition to the heterocyclic ring of purine bases), protein N-glycosylation (dolichol), protein prenylation (farnesyl and geranylgeranyl moieties) and mitochondrial electron transport (ubiquinone), all indispensable for cell survival and steroid hormones such as glucocorticoid/mineralcorticoid, sex steroids, cardioactive steroid hormones, neurosteroids.

The mevalonate is the key intermediate of cholesterol biosynthesis and the precursor of mevalonate synthesis is acetyl-CoA which gives rise to hydroxyl methylglutaryl-Coenzyme A (HMG-CoA). The rate limiting step in this biosynthetic pathway is the conversion of HMG-CoA to mevalonic acid by 3-hydroxy-3-methyl-glutaryl-CoA reductase (HMGR) [7].

1.2 Cholesterol synthesis and homeostasis

The cholesterol biosynthesis is composed of 4 steps (Fig. 3):

1- Synthesis of Mevalonate from acetate.

The first stage in cholesterol biosynthesis leads to the intermediate mevalonate. Two molecules of acetyl-CoA condense to form acetoacetyl-CoA, which condenses with a third molecule of acetyl-CoA to yield the six-carbon compound β-hydroxy-β-methylglutaryl-CoA (HMG-CoA). These first two reactions are catalyzed by thiolase and HMG-CoA synthase, espectively. The cytosolic HMG-CoA synthase in this pathway is distinct from the mitochondrial isozyme that catalyzes HMG-CoA synthesis in ketone body formation. The third reaction is the committed and rate-limiting step: reduction of HMG-CoA to mevalonate, for which each of two molecules of NADPH donates two electrons.

2- Conversion of mevalonate to two activated isoprenes units.

3- Condensation of six activated isoprene units to form squalene.

4- Conversion of squalene to the four-ring steroid nucleus.

A decrease in HMGR activity can regulate the output of the overall pathway without accumulating unusable intermediates.

The liver is considered to be the metabolic power station of mammalians. Therefore, the body relies on a complex homeostatic network to modulate the availability of cholesterol for tissues. This network operates on both the cellular level, mainly in the liver, and within the plasma compartment. The liver is the principal site for cholesterol homeostasis maintenance carried out in many mechanisms.

Cholesterol homeostasis maintenance is carried out by (Fig. 4):

- **biosynthesis, *via* 3-hydroxy-3-methylglutaryl coenzyme A reductase activity;**
  Two moles of acetyl-CoA are condensed in acetoacetyl-CoA that, with a third mole of acetyl-CoA is converted to HMG-CoA. HMG-CoA is converted to mevalonate by HMGR. The reaction catalyzed by HMGR is the rate limiting step of cholesterol biosynthesis, and this enzyme is subject to complex regulatory controls as discussed below.
- **uptake through low density lipoprotein receptors** (LDLr);
  Cholesterol can be taken up through a classic example of receptor-mediated endocytosis by hepatocytes. LDLr plays an important role in cholesterol homeostasis since it binds plasma LDL particles, thus lowering plasma cholesterol levels. This receptor was first discovered in cultured human fibroblasts. Later on,

genetically and immunologically identical receptors were also identified in the liver [8];

- **lipoprotein release in the blood**;

  The cholesterol pool obtained from *de novo* synthesis by hepatocytes can be enzymatically esterified by Acyl-CoA-cholesterol acyl transferase (ACAT) and incorporated into very low density lipoproteins (VLDL), which are then secreted into the bloodstream for transport to peripheral tissues. Cholesterol synthesis in the peripheral tissues also contributes to the hepatic cholesterol pool through the transfer of cholesterol to the liver in a process mediated by high density lipoprotein (HDL) particles (known as reverse cholesterol transport). Dietary cholesterol is also transferred from the intestine to the liver by high density lipoproteins HDL; all HDL particles are internalized in the liver, interacting with the hepatic scavenger receptor (SR-B1) [9];

- **storage by esterification;**

  LDL cholesterol internalized by nonhepatic tissues can be used for hormone production, cell membrane synthesis, or stored in the esterified form.

- **degradation and conversion into bile acids;**

  The hepatic cholesterol may be converted into bile acids, secreted into the intestinal lumen and then eliminated through the feces [10, 11].

1.3 Plasmatic lipoproteins and diseases

There are five major lipoproteins, each of which has a different function. Lipoproteins are a combination of lipid (cholesterol, cholesterol esters, phospholipids and triglycerides) and proteins. Lipids do not travel in the blood by themselves, but they are carried through the bloodstream as lipoproteins. The fatty substances, insoluble in an aqueous environment, may in fact be transported in the blood stream only if linked to specific lipoproteins. The proteic component surface, isolates from environment plasma the components hydrophobic:

- **Chylomicrons;**

Chylomicrons are very large particles that carry dietary lipid. They are associated with a variety of apolipoproteins, including A-I, A-II, A-IV, B-48, C-I, C-II, C-III, and E.

- **Very low density lipoprotein;**

Very low density lipoprotein (VLDL) carries endogenous triglycerides and to a lesser degree cholesterol. The major apolipoproteins associated with VLDL are B-100, C-I, C-II, C-III, and E. The general contribution of hypertriglyceridemia to coronary risk remains uncertain.

Hypertriglyceridemia tends to be associated with low HDL levels; as a result, any apparent increase in coronary disease may be due to the reduction in HDL rather than the elevation in triglycerides [12].

- **Intermediate density lipoprotein;**

As more and more triglycerides are removed from the VLDL because of the action of lipoproteinlipase enzyme, the composition of the molecule changes, and it becomes intermediate-density lipoprotein (IDL).

It is associated with apolipoproteins B-100, C-III, and E. Although LDL is accepted to be the major risk factor in the progression of atherosclerosis, the measurement of LDL also includes IDL. Several studies have shown that serum IDL concentrations are predictive of an increase incidence of coronary heart disease [13].

- **Low density lipoprotein;**

Low density lipoprotein (LDL) carries cholesterol esters and is associated with apolipoprotein B-100. LDL, contain a core of cholesterol esters, lesser amounts of triglyceride, and are enriched in apolipoprotein B-100, which is the ligand for binding to the apo B/E receptor. LDL can be internalized by hepatic and nonhepatic tissues. The internalization of LDL, through the LDL receptor, is regulated by cellular cholesterol requirements via negative feedback control of expression [5]. Cells in positive cholesterol balance, for example, suppress expression. On the other hand, decreased activity of HMGR, the enzyme that controls the rate of *de novo* cholesterol synthesis by the cell, leads sequentially to a fall in cell cholesterol, increased expression of enhanced uptake of cholesterol from the circulation, and a reduction in the plasma cholesterol concentration. Circulating LDL can also enter macrophages and some other tissues through the unregulated scavenger receptor. This pathway can result in excess accumulation of intracellular cholesterol and the formation of foam cells which contribute to the formation of the atheromatous plaque. Circulating LDL that is not taken up, can also enter macrophages through unregulated scavenger receptors [14].

- **High density lipoprotein;**

High density lipoprotein (HDL) also carries cholesterol esters. It is associated with apolipoproteins A-I, A-II, C-I, C-II, C-III, D, and E. HDL, in contrast to LDL and VLDL, has anti-atherogenic properties that include reverse cholesterol transport, maintenance of endothelial function, protection against thrombosis, and maintenance of low blood viscosity through a permissive action on red cell deformability [15, 16]. Reverse cholesterol transport is a process whereby excess cholesterol in cells and in atherosclerotic plaques is removed.

- **Apolipoproteins;**

The major function of the different apolipoproteins can be summarized as follows. Understanding these functions is important clinically, because defects in apolipoprotein metabolism lead to abnormalities in lipid handling.

- A-I — Structural protein for HDL; activator of lecithin-cholesterol acyltransferase (LCAT).
- A-II — Structural protein for HDL; activator of hepatic lipase.
- A-IV — Activator of lipoprotein lipase and LCAT.
- B-100 — Structural protein for VLDL, IDL, LDL; ligand for the LDL receptor; required for assembly and secretion of VLDL [17].
- B-48 — Derived from editig of B-100; required for assembly and secretion of chylomicrons; does not bind to LDL receptor.
- C-I — Activator of LCAT.
- C-II — Essential cofactor for lipoproteinlipase.
- C-III — Interferes with apo-E mediated clearance of triglyceride-enriched lipoproteins by cellular receptors [18]; inhibits triglyceride hydrolysis by lipoprotein lipase and hepatic lipase.
- D — May be a cofactor for cholesteryl ester transfer protein.
- E — Ligand for hepatic chylomicron and VLDL remnant receptor, leading to clearance of these lipoproteins from the circulation; ligand for LDL receptor.

1.4 HMGR: localization and structure

Human HMGR, is an integral glycoprotein resident to the endoplasmic reticulum (ER). The protein consists of a single polypeptide chain which has enzymatic activity and can assemble with other 3 catalytic subunits. Each of the 97-kDa subunits of HMGR is embedded in the ER membrane via a ~350 residue N-terminal noncatalytic region that spans the membrane 8 times [19, 20, 21], whereas the rest of the polypeptide faces the cytosol where it tetramerizes to form the active sites of the enzyme (Fig. 5) [22, 23].

HMGR, catalyzes conversion of HMG-CoA to mevalonate (Fig. 6), the precursor of isoprenoid groups.

Catalysis by this 4-electron oxidoreductase proceeds in three stages, the first and third of which are reductive.

The reaction is: HMG-CoA + 2 NADPH + 2 H^+ → Mevalonate+ 2 $NADP^+$ + CoASH

Catalysis takes place in two sequential hydride transfers from NADPH, in which HMG-CoA is reduced to mevalonate. A protonated histidine residue plays a critical role in catalysis by donating a proton to the thiol anion after the first reduction [24]. Substrate binding induces closure of the COOH-terminal helix, moving the catalytic histidine into position and completing the active site [25, 26].

HMGR has been long-recognized as the rate-limiting enzyme in cholesterol synthesis and as such, is a primary focus of regulation. Mevalonic acid is the central substrate for the production of isoprenoids.

HMGR is a highly conserved enzyme with sequence homologs in eukaryotes, prokaryotes and archaea. Based on sequence alignment of HMGR from eukaryotes, archaea, and bacteria, HMGRs can be categorized into two classes [27, 28]. Eukaryotes and most archaea belongs to Class I. Crystal structures of statin drugs bound to HMGR are available for the Class I human enzyme [29] and for the Class II *Pseudomoonas mevalonii* enzyme.

Class I enzymes utilize NADPH as the electron donor, while class II enzymes utilize NADH.

Archaeal HMGRs vary widely in sequence with enzymes belonging to each class.

The primary sequence element distinguishing the two classes of HMGR is the *cis*-loop, a strictly conserved feature of Class I HMGRs corresponding to amino acids 682–694 of human HMGR [29]. The amino acid sequence of the membrane domain of reductase is strikingly conserved among mammalian species [30], which suggested early on that the region may be important for more than just membrane anchorage. The hydrophobic NH_2-terminus is poorly conserved between the NH_2-termini of fungal and mammalian HMGRs; there is generally less than 25% amino acid identity. The N-terminal domain of reductase is comprised of 339 amino acids and is integrated into ER membranes by virtue of eight membrane-spanning segments that are separated by short loops. The NH_2-terminus of HMGR usually includes a recognizable domain consisting of five consecutive transmembrane spans called a sterol-sensing domain (SSD). The SSD, which is found in other proteins such as the SREBP cleavage-activating protein (Scap) [31] ,may bind lipids and plays an important role in HMGR regulation [7, 21, 32].

The 548-amino acid C-terminal domain of reductase projects into the cytosol and exerts all of the enzymatic activity [22]. The COOH-terminal catalytic domain of Class I HMGRs forms a dimer that comprises the active enzyme and each monomer contributes catalytic residues to form the active site [23, 33]. Expression of the truncated, cytosolic C-terminal domain of reductase produce a stable, catalytically active protein whose degradation was not influenced by sterols [34]. A conserved serine residue corresponding to human HMGR S872 is located

near the active site [35] and S872 phosphorylation reversibly decreases enzyme efficiency. S872 is primarily phosphorylated by the AMP-activated protein kinase (AMPK) in response to a high AMP:ATP ratio [36]. HMGR is dephosphorylated by protein phosphatase 2A (PP2A) [37]. The residue corresponding to human HMGR S872 is not present in Class II HMGRs, nor is it conserved in *Saccaromyces cerevisiae*. However human HMGR S872 is conserved in many other fungi, including the fission yeast *Schizosaccharomyces pombe* [38, 39].

1.5 HMGR function and regulation in mammalian

Feedback regulation of cholesterol biosynthesis was discovered by Rudolf Schoenheimer and Fritz Breusch [40], who observed that mice produce cholesterol in inverse proportion to the amount in their diet. Building on this finding, Marvin Siperstein and M. Joanne Guest [41] determined the target of cholesterol feedback inhibition to be the four-electron reduction of HMG-CoA to mevalonate by the enzyme HMGR.

In mammalian cells, the activity of HMGR, and hence the formation of mevalonate, is controlled through a feedback mechanism mediated by cholesterol that enters cells bound to a plasma lipoprotein, LDL [42, 43]. Intracellular mevalonate levels are finely tuned and tightly regulated by a feedback mechanism that governs the rate HMG-CoA reduction into mevalonate, the major rate-limiting step for the entire pathway [41]. Subsequent experiments showed that this well-understood control mechanism constituted only one part of the HMGR story.

Recent advances revealed that HMGR is regulated at the levels of transcription, translation, post-translational modification and protein degradation.

Transcriptional regulation.

The membrane-bound transcription factor sterol regulatory element-binding protein (SREBP) controls HMGR transcription [31]. SREBP forms a complex in the reticulum endoplasmic (ER) membrane with another integral membrane protein: SREBP cleavage-activating protein (Scap). In cholesterol-replete cells, the inactive SREBP–Scap complex resides in the ER membrane. When cholesterol is depleted, the complex is transported to the Golgi apparatus in COPII vesicles [44]. ER-to-Golgi transport of SREBP requires Scap, which has a COPII recognition site in its NH_2-terminal domain. In the Golgi, SREBP is activated by two sequential proteolytic events that cleave the NH_2-terminal transcription factor domain from the membrane, allowing it to enter the nucleus and activate HMGR transcription [45].

Once synthesised, SREBP is associated with the ER membrane where they remain transcriptionally inactive. In the ER, the SREBP C-terminus interacts with the *cargo* protein Scap which functions as a sterol sensor [45]. In sterol-deprived cells, Scap binds SREBPs and escorts them from the ER to the Golgi apparatus where SREBPs are proteolytically processed to yield active fragments that enter the nucleus and induce the expression of their target genes (e.g., *LDLr, HMGR*). On the other hand, when intracellular sterol content increases, Scap binds the insulin induced gene protein, which keeps the Scap/SREBP complex into the ER, thus blocking the transcription of cholesterogenic genes [45]. This intricate mechanism of regulation is at the root of cholesterol homeostasis maintenance. A major advance in understanding the molecular basis for HMGR sterol feedback inhibition was the discovery of an ER-resident protein called Insig.

Insig binds to Scap in sterol-replete conditions, altering Scap structure and rendering its COPII-recognition sequence inaccessible. This prevents the SREBP–Scap complex from being loaded into COPII vesicles, thereby preventing proteolytic activation of SREBP in the Golgi [44]. Insig dissociates from Scap when sterols are depleted, allowing transport of SREBP–Scap to the Golgi and proteolytic SREBP activation. In addition to its role in regulating HMGR transcription through SREBP, Insig also regulates HMGR degradation (Fig. 7) [46].

Phosphorylation

HMGR is also regulated by cellular metabolic state through an Insig-independent mechanism that is thought to help the cell optimize ATP expenditure during metabolic stress (Fig. 8).

AMP allosterically activates AMPK. Because ATP and AMP compete for the same binding site, AMPK is able to respond to a high AMP:ATP ratio by increasing its catalytic activity. Once activated, AMPK phosphorylates HMGR at a conserved residue in the enzyme active site corresponding to serine 872 of human HMGR. The mechanism by which phosphorylation inhibits HMGR activity has not been conclusively determined, but phosphorylation of S872 may either decrease HMGR affinity for NADPH or interfere with closure of the COOH-terminal flap over the active site [23, 25]. Dephosphorylation of HMGR fully restores enzyme activity (Fig. 8). Protein phosphatase 2A (PP2A), the enzyme primarily responsible for dephosphorylating HMGR *in vivo*, has diverse functions including cell cycle control, viral infection, cell morphology and development [47]. Along with AMPK, PP2A may play an important role in regulating HMGR activity through phosphorylation. However, there is no known physiological role for PP2A regulation in controlling HMGR activity.

Degradation

The degradation of HMGR is mediated by the ubiquitin-proteasome system [48] and mandates, at least, the participation of either one of the polytopic ER Insig proteins [49]. These proteins are thought to couple in a sterol-regulated manner between HMGR and a membrane-bound E3 protein ubiquitin ligase, reported to be gp78 [50]. Thus, degradation of HMGR may be viewed as a special case of the more general cellular quality control mechanism, known as ER-associated degradation (ERAD) (Fig. 9).

This mechanism protects against proteotoxicity by eliminating aberrant proteins from the ER [51]. ERAD also rids the cell of normal ER proteins when they are no longer needed under specific developmental or metabolic circumstances [52]. En route to proteolysis by the cytoplasmic 26S proteasome, HMGR is ubiquitylated on two lysine residues (Lys^{89} and Lys^{248}) within the membrane region and extracted from the ER, along with the short-lived Insig-1, as an intact full-length polypeptide [53]. The ATPase activity of AAA-ATPase p97 provides the driving force for the extraction of HMGR, a step considered to be the hallmark of ERAD known as retrotranslocation or dislocation.

Accelerated ubiquitin-dependent degradation of HMGR in mammalian cells can be elicited not only by sterols (lanosterol, cholesterol, and hydroxysterols) but also by tocotrienols [54] and synthetic bisphosphonate esters, such as SR-12813 and Apomine [55], which bear no structural resemblance to sterols. Importantly, none of these elicitors stimulate the turnover of HMGR in cells that are acutely deprived of mevalonate (*e.g.* by blocking HMGR activity with high concentrations of statins). Evidence supporting a major role for the ubiquitin-proteasome pathway in sterol-accelerated degradation of reductase was first provided by the observation that proteasome inhibition blocks the process, leading to the accumulation of ubiquitinated forms of reductase on ER membranes [56].

1.6 HMGR function and regulation in yeast

Like mammalian cells, yeast cells require sterol as a structural component of their membranes. In yeast, ergosterol fills this role. Ergosterol is structurally similar to cholesterol, but ergosterol contains double bonds between carbons 7–8 of the B ring and carbons 22–23 of the side chain, and methylation of carbon 24.

The similarity between these molecules is enough to allow cholesterol to substitute for ergosterol in the membranes of *Saccharomyces cerevisiae* cells [57, 58].

Correspondingly, yeast produce ergosterol in a biosynthetic pathway that shares most enzymatic steps with its mammalian counterpart [59].

The budding yeast *S. cerevisiae* encodes two HMGR genes, designated *HMG1* and *HMG2*. Presumed to be derived from a single ancestral HMGR by gene duplication [60], Hmg1p and Hmg2p have 62% overall amino acid identity to each other. Their NH_2-terminal membrane domains are 44% identical, and their COOH-terminal catalytic domains are 95% identical. Either gene can supply the essential HMGR activity when the other is deleted [61]. Hmg1p is a stable protein, whereas Hmg2p is rapidly degraded [62]. Although both enzymes are controlled by feedback inhibition, they are regulated in different ways.

Hmg1p is the primary source of HMGR activity during aerobic growth of *S. cerevisiae*. Aerobic growth, promotes synthesis of heme, which activates the transcription factor Hap1p. Hap1p activates *HMG1* transcription, resulting in a 10-fold increase in HMGR activity [63]. Simultaneously, aerobic growth represses *HMG2* expression by an unknown mechanism. Hmg1p is also regulated at the level of translation by a negative feedback system. Mevalonate-starved cells accumulate Hmg1p protein and show an increase in HMGR activity, even as *HMG1* mRNA transcript levels remain unchanged [64]. Translational control of HMG1 expression requires the HMG1 5′-untranslated region so as a lacZ reporter gene was similarly regulated when controlled by the HMG1 promoter. The molecular signal regulating Hmg1p translational control may be mevalonate itself, although the mechanism by which it acts awaits discovery. Like mammalian HMGR, *S. cerevisiae* Hmg2p is regulated by protein turnover through endoplasmic reticulum-associated degradation (ERAD), utilizing the machinery of the HMG-CoA reductase degradation (HRD) pathway. Indeed, regulated ubiquitination of HMGR was initially described in yeast [65]. Hmg2p is recognized and ubiquitinated by the multi-subunit, membrane-associated HRD complex [66]. The membrane-spanning E3 ligase Hrd1p, together with the E2 ubiquitin conjugating enzyme Ubc7p, ubiquitinates Hmg2p. Hmg2p is then extracted from the membrane and degraded by the proteasome.

1.7 Hypocholesterolemic drugs: Statins

As described above, the decrease of intracellular cholesterol leads to a homoeostatic response which induces up-regulation of cell-surface receptors that bind atherogenic lipoproteins, which are taken up into cells and degraded. Thus, the reduction of hepatic cholesterol synthesis via HMGR inhibition is an attractive approach for the treatment of dyslipidemia. Statins, strong HMGR inhibitors (Fig. 10), are widely used in therapies against hypercholesterolemia and they are available or in late-stage clinical development. Statin

treatment strongly reduces mevalonate production and, as a consequence, hepatic cholesterol biosynthesis (Fig. 11).

Considering that plasma cholesterol increase is the main cause of cardiovascular disease, cholesterol biosynthesis *via* HMGR and uptake *via* LDLr are the targets of hypercholesterolemia treatment. Statins, able to inhibit intracellular cholesterol synthesis and, as a consequence, to increase LDLr membrane exposure, have been considered the golden standard against hypercholesterolemia. Nevertheless, since disruption of cholesterol homeostasis can be ascribable to other factors in addition to HMGR and LDLr deregulation, the current editorial highlights how hypercholesterolemia treatment should be supported by a specific diagnosis and, in turn, adapted to the identified causes of plasma cholesterol increase.

HMGR activity is tightly regulated to ensure maintenance of lipid homeostasis, disruption of which is a major cause of human morbidity and mortality. New insights into the branched pathway of mevalonate metabolism have been made possible in the late 1970s through the use of compactin, a fungal metabolite that is also known as ML236B. In 1976, Endo, Kuroda, and Tanzawa [67], isolated compactin and made the fundamental observation that this compound is an extremely potent competitive inhibitor of HMGR. Incubation of cultured cells with compactin blocks mevalonate production [68, 69], and converts the cells into mevalonate auxotrophs.

Inhibition of HMGR has been proven to be one of the most effective approaches for lowering plasma LDL level and reducing cardiovascular event rates. As part of a compensatory mechanism to cholesterol depletion in the liver, inhibition of HMGR leads to the increased production of this enzyme and of low-density lipoprotein receptors (LDLR), this latter process give a subsequent clearance of LDL from systemic circulation.

Statins inhibit the endogenous cholesterol biosynthesis in hepatocytes, thereby increasing the transcription of HMGR and LDLR genes.

Statins bind directly to the HMGR active site and are competitive inhibitors of the enzyme with respect to HMG-CoA [69]. All statins have structural similarity to the 3-hydroxy-3-methylglutarate moiety of HMG-CoA and occupy the HMG-CoA binding pocket of HMGR (Fig. 11), [26]. The remainder of the statin molecule is rigid, hydrophobic and highly variable among different statins. This part of the molecule makes contact with residues in the active site, but does not occupy the NADPH binding site.

Accordingly, statins do not interfere with NADPH binding to HMGR.

1.8 Side effects of statins

As described above, the decrease of intracellular cholesterol leads to a homoeostatic response which induces the up-regulation of cell-surface receptors that bind atherogenic lipoproteins, which are taken up into cells and degraded. Thus, the reduction of hepatic cholesterol synthesis *via* HMGR inhibition is an attractive approach for the treatment of dyslipidemia.

Statin treatment strongly reduces mevalonate production and, as a consequence, hepatic cholesterol biosynthesis.

Although these drugs are generally well tolerated, statins can lead to several side effects, the most frequent is myopathy. Statin-associated myopathy is characterized by a wide spectrum of symptoms, ranging from myalgia up to life-threatening rhabdomyolysis [70, 71].

These adverse effects could be ascribable to the decrease of some HMGR end-products such as prenyls or ubiquinone [72].

Although statins are the largely prescribed HMGR inhibitors, because they are surely safer, well tolerated, and highly efficient in reducing LDL levels, cardiovascular disease remains the main cause of mortality in westernized 4 countries.

The pursuit of novel therapies to target the residual risk is focused on raising HDL levels [73].

1.9 Citrus bergamia Risso

Some natural compounds found in our diet have been shown to possess therapeutic and pharmacological properties. In particular, studies conducted by daily administration of citrus fruit juice have shown that this practice positively influences plasma lipid levels and that it can be associated with reduced risk of coronary heart disease [74].

Literature data, show that the hypolipidemic effects can be correlated to several components of citrus juices, such as flavonoids (naringin and hesperidin), pectins and ascorbic acid, which have a high antioxidant potential and they can interfere with cholesterol metabolism [75, 76].

Bergamot is the common name of the fruit Citrus bergamia Risso, which belongs to the family Rutaceae, subfamily Esperidea. A peculiarity of this fruit is the considerable abundance and variety of nutraceuticals, such as naringin, neoeriocitrin, and neohesperidin, which are present in the juice on the order of hundreds of ppm.

In addition of naringin and hesperidin other flavonoids, such as rhoifolin, neodiosmin and some chryosoeriol derivatives are present in smaller amounts [77, 78, 79]. Different tissues of this fruit also produce the flavonoids diosmin and poncirin [80]. Moreover, some statin-like components such as brutieridin and melitidin [81] are present in bergamot fruit juice, these

substances may play a significant role in the anticholesterolemic activity known in the local folk medicine [82].

The uniqueness of bergamot trees, is represented by a habitat that is virtually restricted to the coastal region of the Ionian Sea in the southern Calabrian region of Italy.

Hence, the production of bergamot has been a flagship product of Calabrian agriculture for many years, and its volatile fraction is still used in the cosmetic and perfumery industries, despite the presence on the market of synthetic surrogates.

Bergamot juice has not reached the popularity of other citrus juices in the daily diet for its organoleptic properties, but it is used to fortify fruit juice in place of synthetic additives.

Apart from the well-known components of the fruit of *C. bergamia* thoroughly investigated in the last three or four decades, a detailed profiling of bergamot extract by tandem mass spectrometry (MS/MS) has led to the discovery of some flavonoid diglycosides carrying the 3-hydroxy-3-methylglutaric acid (HMG) moiety. In the present study, two new molecules have been isolated and identified as HMG conjugates of neohesperidin and naringin [81] namely, brutieridin (1, hesperetin 7-(2"-R-rhamnosyl-6"-(3""- hydroxy-3""-methylglutaryl)-β-glucoside)) and melitidin (2, naringenin 7-(2"-R-rhamnosyl-6"-(3""-hydroxy-3""-methylglutaryl)-β-glucoside)). The purified powder of brutieridin and melitidin is reported in the following text as brutieridin and melitidin fraction: BMF (Fig. 12).

METHODS

2.1 Purification of brutieridin and melitidin

A dry extract of bergamot fruit (Citrus Bergamia Risso) provided from Gioiasucchi s.r.l. (Gioia Tauro, Italy) was submitted to flash chromatography using the VersaFlash™ system from Supelco (Saint Louis, MO); 35 g of C 18 200-400 mesh (Aldrich, Saint Louis, MO) was used as stationary phase into a 40 x 37.5 mm column. The column was activated eluting in sequence 200 mL of EtOH, 200 mL of H 2 O/EtOH (50:50), 200 mL of H 2 O/EtOH (75:25), 200 mL of H 2 O/EtOH (87.5:12.5), and finally 500 mL of H 2 O, maintaining the flow rate at 25 mL/min.

The column was loaded pouring 2 g of dry extract dissolved in 10 mL of H 2 O with a syringe; 100 mL of water was then eluted at 5 mL/min and the flow rate was gradually increased to 50 mL/min. The elution of the components of the dry extract was conducted using 4 L of H 2 O collecting fraction of 0.5 L each, then 1 L of H 2 O/EtOH (90:10) and 500 mL of H 2 O/EtOH (70:30) were used collecting fraction of 50 mL each. The first two fractions collected from the elution step using H 2 O/EtOH (70:30) were combined and evaporated to dryness under vacuum. 125 mg of a mixture containing 50% of brutieridin and 12% of melitidin (Fig. 12), were obtained in a single run. All fraction were monitored using a FractionLynx semi-preparative system from Waters (Milford, MA) in analytical mode equipped with an UV detector and a Luna C 18 column 5 mm particle size, 25 cm × 4.6 mm (Supelco, Saint Louis, MO). The run time was 105 min, while the flow rate was set at 1 mL/min and the following eluents and gradient conditions were used: 0.1% HCOOH in H 2 O (solvent A) and CH 3 OH (solvent B); 10 min isocratic 80% A; 2 min linear gradient from 80% to 74% A; 65 min linear gradient from 74% to 31% A; 18 min linear gradient from 31% to 80%; 10 min isocratic 80% A. 20 ml of each fraction were injected into the loop, while the Absorption wavelength of the UV detector was set at 280 nm [81].

2.2 Animals and diets

Male Wistar strain rats, weighing about 150 g each, were purchased from CharlesRiver (Lecco, Italy). The study was approved by the Italian Ministry of Health (permission number 100000136 released by Italian Ministry of Health in date 02-09-2010). Animal experiment protocols followed the institutional guidelines of the Italian Ministry of Health for Animal Care (D.M. 116/1992). Animals were housed 1rat per cage in an air conditioned room having a 12 h light–dark cycle and with ad libitum access to food and water. Before the experiment,

all the animals were allowed to stabilize by being fed with regular rodent chow, then they were randomly divided into four groups of twelve animals each:

• Group I (hypercholesterolemic controls) received the hypercholesterolemic diet (5% of cholesterol) for 3 weeks.

• Group II received the hypercholesterolemic diet (5% of cholesterol) for 3 weeks; from the 2nd to the 3rd week each rat was administered by gavage with simvastatin (20 mg/kg bw/day).

• Group III received the hypercholesterolemic diet (5% of cholesterol) for 3 weeks; from the 2nd to the 3rd week each rat was administered by gavage with the BMF (60 mg/kg bw/day).

Regular and hypercholesterolemic diets were supplied by Charles River (Lecco, Italy), simvastatin was purchased from Sigma Aldrich (Milan, Italy). During the experiment rats were weighed daily and the 24 h food consumption was recorded. At the end of the study, the animals were killed by decapitation and 14 blood samples were collected in EDTA-treated tubes, centrifuged at 2500g for 15 min and the serum was separated and stored at -20°C until analyze [83]; liver was excised and immediately frozen in liquid nitrogen, then stored at -80°C until use.

2.3 Biochemical estimations

The livers were cut into small pieces, washed several times in a cold buffer (0.25 M sucrose, 3 mM EDTA, 20 mM Tris–HCl, pH 7.0), next they were homogenized in the same buffer and treated as described [84] for TC extraction.

Briefly, an aliquot of 10 mg protein sample was saponified with alcoholic KOH for 90 min at 85–90 °C. Nonsaponifiable constituents were extracted 3 times (5 mL each) with light petroleum (b.p. 40-60°C). The pooled extracts were then evaporated to dryness under N 2 and the residue was dissolved in 2-propanol. Total lipids were extracted from liver homogenate (10 mg protein) using chloroform/methanol (1:1 v/v) according to [85].TG, TC, HDL, LDL levels were evaluated by direct enzymatic assays using Trigliceridi Kit, Colesterolo kit (Chematil srl Salerno, Italy), HDL Kit (Intermedical srl Naples, Italy) and LDL Kit (Biogemina srl Catania, Italy), respectively, according to manufacture's instruction.

2.4 RNA isolation, reverse transcription and real-time PCR

RNA extraction, reverse transcription and quantitative real-time polymerase chain reaction RNAs were extracted from liver samples using the Aurum Total RNA mini kit (Bio-Rad

laboratories, Milan, Italy) according to manufacturer's instruction. Total RNA (1 µg) isolated from liver was reverse-transcribed with RNA PCR core kit (Applied Biosystems, Monza, Italy) using random hexamers as primers (final volume, 20 µl).15 The reverse transcription reactions were conducted at 42°C for 30 min and then inactivated at 95°C for 5 min. Quantitative real-time polymerase chain reaction (RT-PCR) was performed with the obtained complementary DNAs (cDNAs) using the Applied Biosystems StepOne™ Real-Time PCR System (Applied Biosystems, Monza, Italy). Primers based on the cDNA sequences of the genes of interest were designed using Primer Express (Applied Biosystems, Monza, Italy). In each real- time PCR reaction sample (final volume 20 µl) 10 ng of cDNA, 10 µl of the Power SYBR ® PCR Master Mix (Applied Biosystems, Monza, Italy) and 0.3 µL (150 nM) of the primers specific for each analyzed genes were used. Each experiment was repeated at least 3 times. The comparative threshold cycle method was used in relative gene quantification as previously described [86] using 18S gene (for rats) or 35S gene (for yeast strain) as the endogenous control.

2.5 Microsomal fraction extraction and Western blot analysis

The liver homogenate, obtained as previously described, was centrifuged at 800 g for 8 min, pellet was discarded and supernatant was centrifuged for 10 min at 12,000 g. The pellet containing the mitochondrial fraction was discarded and the supernatant was first centrifuged at 20,000 g for 20 min and then at 105,000 g for 60 min in order to obtain the cytosolic fraction and pelleted microsomes. The latter were re-suspended in the homogenizing medium and centrifuged again under the same conditions. Contamination of microsomal preparation by other subcellular fractions, ranging from 5% to 9%, was determined by the assay of marker enzymes as described [87].

2.6 Lipid extraction

Yeast cells were harvested, washed with water, and their wet weight was estimated. Lipids were extracted according to the method of Folch [88] with some modifications.

The cells were homogenized and suspended in chloroform : methanol (2:1). After dispersion, the mixture was agitated for 8 hours at room temperature. The homogenate was centrifuged to recover lipid phase that was used in alkaline hydrolysis of lipids.

2.7 HPLC analysis of total cholesterol in liver samples and yeast samples

The analyses of samples were performed following a method from literature [89]. The analyses were conducted using a HPLC 1100 from Agilent Technologies (Waldbronn, Germany) equipped with an UV detector and a Luna C 18 column 5 µm particle size, 25 cm × 4.6 mm (Supelco, Saint Louis, MO). The flow rate was set at 1 mL/min and the following eluents and isocratic conditions were used: 10% H 2 O, 45% 2-propanol, 45% Acetonitrile. 20 µl of each sample dissolved in 0.4 mL of 2-propanol were injected into the loop in triplicate. The run time was 30 min, while 17 the Absorption wavelength of the UV detector was set at 214 nm. A standard calibration curve was built by injecting standard cholesterol samples in a concentration range from 30 to 950 mg/L.

2.8 Bacteria, yeast strains and recombinant expression plasmids

E. coli TG1 was used for propagation of plasmids. *E. coli Rosetta* was used to express the His 6 –tagged wild-type enzymes.

The human wild-type catalytic fragment amino acids 420-888 of HMGR protein (named cf-HMGR in the following text) was amplified by PCR reactions that involve the use of "nested primer" and performed on human cDNA liver (Hep G2 line cells from ATCC) using two couple of forward and reverse nested oligonucleotides (see table 1) [90]. Based on the sequence of human HMGR obtained from the ncbi database (http://blast.ncbi.nlm.nih.gov/). The amplified DNA was cloned into the bacterial expression vector pET-21b/V5/His, [91]. The sequence of the resulting plasmid named cf-HMGR, was confirmed by nucleotide analysis. The recombinant plasmid pYES2-HMGR was a kind gift of Agata Leszczynska and Anna Szkopinska from Institute of biochemistry and biophysics PAS, Polish Academy of Science, Warsaw, Poland [92, 93].

2.9 Expression and purification of recombinant cf-HMGR

Single colonies of cells harbouring recombinant DNA were picked from plates containing Luria–Bertani medium with ampicillin (100 µg/ml) for inoculation of 5 ml cultures. These cultures were grown overnight at 37°C before use in inoculating 100 ml cultures in Luria–Bertani medium containing ampicillin (100 µg/ml). Cultures were grown at 37°C until DO, measured at 600nm using a UV-spectrophotometer (Jenway Model 7315), reached the 0.7-0.8 value. Isopropil-b-D-tiogalattopiranoside (IPTG), was then added to a final concentration

of 1 mM, and the culture further grown for 3 h. The cells were harvested by centrifugation at 3500 g at 4°C for 10 min and stored at-80°C until use.

For protein extraction, cell pellets were thawed on ice, resuspended in 5 ml of lysis buffer (100mM Sucrose, 50mM KCl, 40mM $K^{+}PO_4^{-}$ pH 7.2, 30mM EDTA, 10mM DTE, 8,3% glycerol) and then lysed by sonication using sonifier branson 250 equipped with a microtip probe (Branson Ultrasonics, Danbury, CT, USA). The program used a power setting of 40% duty cycle for 10 min in a water bath, with pulse of 1 second followed by cooling on ice. Extracts were clarified by centrifugation at 17,000 g for 15 min at 4°C using a centrifuge (Beckman-Coulter, Avanti J-30I, CA, USA).

The supernatant (about 2 mg/ml) was incubated for 1 h at room temperature, than was applied to nickelnitrilotriacetic-agarose (Ni^{2+}-NTA Qiagen, Milan, Italy) preequilibrated with the lysis buffer. The column was washed once with 2 ml of washing buffer 1 (500 mM NaCl, 10mM Pipes pH 7, 1mM Imidazole, 0,1mM PMSF), once with 2 ml of washing buffer 2 (500 mM NaCl, 10mM Pipes pH 7, 5mM Imidazole, 10% Glycerol), once with 2 ml of washing buffer 3 (300 mM NaCl, 10mM Pipes pH 7, 5mM Imidazole, 5% Glycerol), once with 2ml of washing buffer 4 (100 mM NaCl, 10mM Pipes pH 7, 10mM Imidazole, 1% Glycerol), once with 2ml of washing buffer 5 (100 mM NaCl, 10mM Pipes pH 7, 20mM Imidazole), once with 2ml of washing buffer 6 (100 mM NaCl, 10mM Pipes pH 7, 40mM Imidazole). Finally the cf-HMGR was eluted using 5 × 0.2 ml of elution buffer (100 mM NaCl, 10mM Pipes pH 7, 80 mM imidazole). The fractions containing cf-HMGR were pooled and used for next analysis.

2.10 Spectrophotometric assay of cf-HMGR activity

The activity of the solubilized cf-HMGR was determined at 37°C in a total volume of 100 µl. The spectrophotometric assay was conduct by the method described by Kleinsek et al. [94] with a light modification. The assay system consisted of 160mM Potassium phosphate (pH 6.8), 200mM KCl, 4mM EDTA, 10mM DTE, 0,2mM NADPH, 0,1mM HMG-CoA. The reaction was initiated by adding HMG-CoA to the complete assay mixture. The HMG-CoA dependent oxidation of NADPH was monitored in a UV-spectrophotometer (*Applied Biosystems model* Jenway 7315) equipped with a peltier unit adjusted at 37°C. The rate of oxidation of NADPH in the absence of HMG-CoA was subtracted from the rate obtained with substrates.

2.11 Others methods

Protein concentrations were determined by the Bradford method, according to the manufacturer's instructions (Bio-Rad laboratories, Milan, Italy).

Equal amounts of protein (10- 100 µg) were analysed using SDS/PAGE [95] and were resuspended in SDS loading buffer and boiled for 5 min, then resolved on a gel at pH 8.3; the gel was stained with Commassie Blue. The membrane was blocked with Tris-buffered saline/Tween (20 mmol/L Tris (pH 7.6), 150 mmol/L NaCl, and 0.1% Tween-20) supplemented with 5% nonfat milk for 1 hour at room temperature and then incubated overnight at 4°C with the specific primary antibody. The membrane was washed three times with Tris-buffered saline/Tween buffer and further incubated for 1 hour at room temperature with secondary antibody–horseradish peroxidase conjugate. The protein bands were detected using Western Lightning ™ Plus-ECL kit (Perkin Elmer, Monza, Italy). The same membrane was reprobed with anti-ß-tubulin antibody or anti-GAPDH to confirm the equal loading of proteins prepared from liver after different treatments. Antibodies anti-HMGR (H-300), fatty acid synthase (FASN,H-300), LDL receptor (C-20) and anti-ß-tubulin (D-10), anti-GAPDH (FL-335) were supplied by Santa Cruz Biotechnology (CA, USA) and used following the manufacturer's instructions. The anti-peptide antibodies raised in rabbit (Thermo Sientific) against a peptide corresponde to amino acids 700-888 (single letter coding) of HMGR.

2.12 Statistical analysis

All data were presented as means ± SD for the number of experiments indicated in each case. Data were analyzed by Student's t-test using the GraphPAD Prism4 software (GraphPad Software, USA). Differences were considered statistically significant at $P<0.05$.

RESULTS

In this study we examined the hypolipidemic action of the natural compound BMF, extracted from bergamot fruit, on the lipid metabolism using two different in vivo systems and one in vitro system.

In the first system we used the rat as model organism to investigate the changes in lipoprotein composition, metabolism and transport as consequence of the HMGR inhibition.

In the second system we used the *S. Cerevisiae*, deleted of the two yeast HMG genes and transformed with the full-length human HMGR, in order to evaluate the changes in sterol content.

Furthermore, we set up an in vitro system consisting of the expression of the catalytic fragment of the human HMGR in *E. coli* useful for a rapid and easy screening of different statin-like molecules.

3.1 Food intake and body weight gain

The data on food intake and body weight are shown in figures 13, 14. In figure 13 it is summarized the daily food intake in respect to the whole study period for each group of rats. As positive treatment control in rats we used one of the most prescribed statins among people, simvastatin. No significant differences in food intake were observed for each hypercholesterolemic group (i.e. simvastatin or BMF treated rats versus untreated). Figure 14 shows the overview of changes in body weight over the study period for the different rat groups. For each rat the body weight normally increased during the study period, without significant differences in weight within the same group or between the different groups. Moreover, the livers excised from each treated group rats were not significantly different in weight from those of the induced rats (data not shown). These observations indicate that the diet and treatments used in this study were well tolerated in rats, given that no physical alteration, body weight loss or food intake reduction occurred over the period of the study. A group of normally fed rats was taken under evaluation as control to verify the induced hypercholesterolemia (data not shown). As shown in figures 13, 14 no significant difference among groups has been found, thus both hypercholesterolemic diet and drugs treatment seem to be well tolerated by rats. Additionally, rats fed on hypercholesterolemic chow show a significant increase in TC serum concentration in respect to the normal fed group (data not shown), indicating that our hypercholesterolemic model is correctly obtained.

3.2 Effect of simvastatin and BMF on serum and hepatic lipid content

We used a colorimetric assay to examine the concentrations of TC, LDL, HDL and TG in rat serum, whereas the hepatic TC and TG contents were measured by HPLC and colorimetric assay respectively. In serum samples the hypercholesterolemic groups treated respectively with simvastatin (H+S) and with BMF (H+BMF) exhibited a significant decrease of TC (of about 30% and 20% respectively) in respect to the untreated hypercholesterolemic group (H) (Fig. 15, panel A). In liver samples, we observed a reduction in TC content of 11% for simvastatin treated rats and a more significant reduction, of 35%, under BMF treatment (Fig. 15, panel B). It is well known that an elevated plasmatic concentration of LDL is associated with a high risk of coronary heart disease and atherosclerosis plaque lesions, thus we also investigated whether there were changes in LDL concentrations. A significant reduction of LDL content was measured in H+S (24% lower) and H+BMF (40% lower) groups (Fig. 16, panel A). Conversely, no significant difference in HDL levels was found in H+S treated group, whereas, surprisingly, a significant increase was observed in H+BMF treated rats group (20% higher) in respect to the H control group (Fig. 16, panel B). Since HMGR inhibitors have been shown to contribute in decreasing serum triglycerides levels in experimental animals, we investigate this feature in our model. We measured serum and hepatic triglycerides content (Fig. 17), demonstrating that in both cases there was a decrease in simvastatin and BMF treated rats, in respect to the untreated group, the decreases were of about 32% and 20% respectively for serum TG (Fig. 17, panel A) and of about 18% and 35% for hepatic TG (Fig. 17, panel B). observing a decrease of TC, LDL and TG levels in simvastatin treated rats (Figs. 15, 16, 17), whereas no significant variation of HDL levels has been observed (Fig. 16). Most importantly, TC and TG levels have been found decreased also in BMF treated rats, but in a lower extent in respect to the simvastatin group (Figs 15, 17), whereas the ability in decreasing LDL levels seems to be higher respect to the simvastatin (Fig. 16). Notably, these results come together with another clinically important effect, i.e. a significant increase in HDL levels (Fig. 16). It is long since known that the main class of lipoproteins involved in many vascular diseases is really represented by LDL, on the contrary it is well-known that an increase of HDL exerts a protective effect with regard to these diseases. In this regards it must be outlined that the observed drop in LDL serum levels is accompanied by an increase of HDL contents exclusively in BMF treated rats group. The latter peculiarity represents a favourable event, given that HDL are able to picking up cholesterol from peripheral tissues or cells and to carry it back to liver, where they are readily

catabolized contributing to decrease the atherosclerosis-associated diseases risk. These outcomes indicate that BMF could be a high potential control agent in hypercholesterolemia caused diseases. Since serum TC and TG levels are depending on their biosynthesis, which mainly occurs in liver, we also investigated their hepatic levels (Figs 15, 17). We found a decrease in TC and TG in simvastatin treated rats and, in a surprisingly higher extent, in BMF treated group suggesting that hepatic metabolism of TC and TG is affected by drugs treatment. These observations led us to deduce that the decreased lipidic content in serum is correlated with the decrease in TC and TG synthesis and to their secretion by liver. Additionally, it is well known that changes in serum and hepatic lipidic contents caused by drugs supplementation are strictly related to variation of hepatic key enzymes and proteins involved in TC and TG metabolism.

3.3 Effect of simvastatin and BMF administration on hepatic HMGR, LDLR and FASN mRNAs and protein levels

In order to investigate the molecular mechanisms of BMF in hypercholesterolemic induced rats, we evaluated the transcriptional levels of two main proteins involved in cholesterol metabolism, as HMGR and LDLR and the expression of the main enzyme involved in fatty acid biosynthesis, i.e. FASN. As shown in Fig. 18, simvastatin and BMF showed a similar behaviour on gene expression of the above mentioned proteins. Particularly, simvastatin administration, respect to untreated control, brought to an increased gene transcription of HMGR, LDLR and FASN genes in an extent of 1.45, 1.83 and 1.33 fold respectively. As well BMF treatment increased the expression of HMGR, LDLR and FASN genes of 1.66, 1.56 and 1.80 fold respectively. In all cases, mRNAs increase was appreciable respect to the untreated hypercholesterolemic group. The data obtained by RT-PCR on hepatic mRNA levels were additionally verified by Western blot analyses, conducted on the microsomal or cytoplasmic fractions or on the total cells extract obtained from rats liver of each experimental group, considering the different sub- localization of proteins analyzed. As shown in Fig. 19, in accord to RT-PCR results, the administration of simvastatin and BMF to the hypercholesterolemic rats led to a clear increase of HMGR, LDLR and FASN proteins in respect to the untreated rats.

3.4 mRNA level and lipid profile of yeast strain encoding human HMGR

Simultaneously to rat system, in a yeast strain engineering to express the human HMGR full-lenght, we have measured the changes in mRNA level of human HMGR and in the yeast

sterol content in order to confirm the data previously obtained in rat system.

The literature data [96] indicate that in an inhibition of the enzyme activity HMGR corresponds to an increase of its transcript. This apparent anomaly is justified by the existence of a compensatory mechanism. In order to compensate for the lack of enzyme activity, cells induces an increase in its transcription.

To determine the expression levels of the human HMGR gene, we carried out a quantitative real time RT-PCR analysis on total RNA samples extracted from different yeast cultures growth in standard medium unsupplemented or in medium supplemented with pravastatin (a statin available in active form) or with BMF. The data obtained show, that the mRNA levels of the enzyme HMGR increase (Fig. 20). In the first 24 hours the increase is recorded mainly as a result of treatment with pravastatin 50 ug/ml (Fig. 20 A) while no significant effect was observed with BMF 50 ug/ml. At 48h the pravastatin maintains a constant action, without significant variations over time while BMF action appeared evident (fig.20 B). These data may suggest an action time-dependent for BMF.

The inhibition of enzyme determine a reduction of production of mevalonate that results in a decrease of the pool of sterols that converge on the formation of ergosterol, analogue of cholesterol in yeast. Specifically, there was a drastic reduction of lipidic content into treated cells. To examine if changes in human HMGR gene expression level after of pravastatin and BMF treatment, influence the lipid metabolic pathways, we analyzed the total lipids extracted from yeast cells expressing the wild-type form of human HMGR gene. As shown (Fig. 21) in all cells that were growth in the presence of pravastatin and BMF we noticed a significant drop in the level of sterols. Surprisingly the drop of the lipidic pool was evident since 12 h of treatment with pravastatin or BMF, these results were also confirmed after 24 and 48 hours (Fig. 21). BMF has been shown to have hypolipidemic activity similar to commercial pravastatin.

3.5 Cloning of recombinant plasmid cf-HMGR

Finally, we have set up an in vitro system based on the expression of catalytic fragment of human HMGR in *E. coli*. The bacterial model was chosen for its versatility and ease of use. The data collected were employed to obtain information about BMF. Furthermore, we think that this system could be used as tool in the future for a rapid screening of different statin-like compounds or HMGR inhibitors.

With this aim, starting from the sequence of the human HMGR mRNA (accession number NM_000859) we cloned the fragment corresponding to catalytic region of enzyme (amino

acids 420-888) in the pET-V5-His expression vector. The catalytic coding region for the hHMGR was amplified from first strand liver cDNA (100 ng) by polymerase chain reaction with nucleotides based on the sequence of mRNA clone (see table 1).

To verify that the reaction had occurred, it has been loaded on the agarose gel, with the marker 1 Kb Ladder. The result has been a large band around 1407 bp. We proceeded to the digestion of the cDNA and plasmid with restriction enzymes Nde I and Bam HI. Subsequently has been carried out a ligation reaction to obtain the recombinant plasmid cf-HMGR with the insert.

3.6 Expression of the soluble fragment of cf-HMGR in Escherichia coli cells

We moved to the over-expression of the cDNA coding for the catalytic fragment of the human HMGR in Rosetta *E.coli* strain. The over-expression of the recombinant cf-HMGR was monitored over time. After induction, there was an expression band, around 53 kDa in correspondence of the lane loaded with the inclusion bodies (IB). The band at about 53 kDa, in agreement with what is expected becomes more and more intense in samples taken at one hour, and then two to three hours after induction. The same observation can't be done to the gel loaded with the supernatants obtained from cell lysates. Any over-expression band was observed in the sample control. To confirm the expression of the recombinant protein cf-HMGR, an aliquot of cell lysate extracted from *E.coli* cells transformed with the recombinant vector, was loaded on SDS-PAGE and the nitrocellulose membrane was undergoes to Western blot analysis (Fig. 22).

3.7 Extraction of HMGR from E.coli, and spectrophotometric assay of activity

In order to have a quantitative estimate of enzyme activity and to compare the changes in activity in response to the use of inhibitory substances, we chose to use the enzyme in soluble form as an analytical tool to test the effectiveness of the system. To assess the functionality of the catalytic fragment cloned, we choose the spectrophotometric method, which is widely accepted and used in other biochemical studies and more cost-effective compared to tests conducted with the radioactive. All activities are measured in duplicate and compared to a control. The reaction catalyzed by HMGR is NADPH-dependent so we could exploit the oxidation of NADPH to estimate the preceding of the reaction. The change in absorbance was monitored at 340 nm in a time course experiments. The reaction control was conducted in the absence of the substrate HMG-CoA.

After numerous tests we optimized the assay conditions and we got a standard procedure. In subsequent experiments we used pH 6.8 (Fig. 23).

We then conducted experiments in which the mix described above was added of HMG-CoA to analyze the behavior of the enzyme in the presence of the substrate. Each test of activity is expressed graphically showing in an immediate way the progress of the reaction. At the end of each activity assay is estimated the value of enzyme unit.

3.8 Inhibition assay

We compared the changes of the enzyme activity in the presence of inhibitory molecules. The topic is to demonstrate the ability of some substances to interfere with catalysis, reducing it. The tested substances belong to the class of statins, lipid-lowering drugs whose mechanism of action is based on the inhibition of the enzyme HMGR. The molecule used as a selective inhibitor of the enzyme HMGR was pravastatin who shares the chemical and pharmacological properties of the major statins and the pravastatin, widely used as a cholesterol-lowering drug in the therapy of numerous dyslipidemias. Literature data [97] reported a Ki value of 48 nM. We used the pure powder of pravastatin (pravastatin sodium, SIGMA, P4498, 015K4706), to conduct spectrophotometric assays of inhibition. From the results obtained and shown, it is evident that the decrease in absorbance within 10 minutes of the test is proportional to the concentration of pravastatin used (Fig. 24). For very low concentrations between 1 and 10 nM, the decrease in absorbance is comparable to that recorded in the standard reaction conducted in the absence of inhibitor. To concentrations of 20 nM the rate of reduction in absorbance slows registering an initial and significant inhibition of enzyme activity. Increasing concentrations of the inhibitor at 30 and 40 nM is reached and exceeds 50% of enzyme inhibition. For values higher than 50 nM, such as 75, 100 or 500 nM, the inhibition of the enzyme is almost total. The reaction at this point is completely blocked, the functionality of the enzyme is impaired.

The crude extract of cf-HMGR, was tested with BMF to test the inhibition properties of BMF. Our results show that BMF inhibit at 40% the catalytic activity. This inhibition was observed when BMF was used at 25 uM and 50 uM (Fig. 25). In figure 26 is reported the variation of absorbance in kinetics studies conducted with the only brutieridin purified molecule.

The cf-HMGR purified as described in methods 2.2, was used to test the catalytic activity of the purified protein. The purified fractions were pooled and were done the activity assays.

In figure 27, is showed the gel of purification and in figure 28 is reported the variation of absorbance in dependence of the time of incubation of purified protein with the assay buffer.

DISCUSSION

Cholesterol homeostasis is subtly regulated at several levels as, for instance, intestinal absorption, hepatic uptake of LDL, de novo synthesis and excretion. When its blood concentration rises over certain levels, the incidence of atherosclerosis and cardiovascular or cerebrovascular diseases becomes higher. One of the most significant advances in drug therapy during the twentieth century was the development of the statin class of drugs. These agents inhibit the activity of HMGR as well as induce up-regulation of LDLR on cell surface. As such, these drugs are enormously effective in reducing plasma concentrations of LDL. Even though these classes of drugs show a significant reduction in mortality and contribute to ameliorate the clinical conditions, the occurrence of adverse side effects is not a rare event in many patients. Recent studies suggest that a more effective strategy to treat these diseases is a serum LDL decrease associate with a contemporaneous raise of HDL levels. It is also true that, in many cases, a more correct daily diet can prevent the hypercholesterolemia, lowering the risk of the associated-diseases onset or even it can have an anticholesterolemic activity as reported from local folk medicine. Several research studies are focused on the individuation of alternative treatments, either as drugs or diet integrations, which may represent another option for preventing and/or treating the risk of diseases due to the excess of circulating cholesterol. Some studies, conducted on different citrus species, clearly indicate a positive influence of their juice on serum lipid levels probably correlated to the presence of many bioactive compounds as, for instance, flavonoids, pectins, ascorbic acid. Furthermore recent studies have shown the presence of some statin-like compounds in the Citrus bergamia Risso. In the present study, we compare the effect of an enriched fraction obtained from bergamot fruit containing the statin-like coumpounds brutieridin and melitidin in respect to commercial simvastatin on hypercholesterolemic rats.

Cholesterol metabolism has been monitored evaluating the expression level of HMGR and LDLR transcripts and proteins, while triacylglycerol metabolism has been evaluated monitoring the transcript and protein levels of FASN gene involved in fatty acid and then in triglycerides syntheses. We have found an upregulation in HMGR and LDLR genes transcription under simvastatin treatment, according to previously published data and a significant induction in FASN gene transcription (Fig. 18), in respect to the untreated group. Similar results have been obtained in BMF treated group, but in a higher extent. As further demonstration of this positive regulation, we have also observed a correlated increase in

proteins expression of all the three above- mentioned genes in liver, both under simvastatin and BMF supplementation (Fig.19). Whereas simvastatin effects on HMGR and LDLR gene transcription have been already shown, the same effects on FASN gene transcription has not been reported so far and, as well, the significant increase in protein expression has been showed in this paper for the first time and should be taken into account in the simvastatin physiological effects knowledge. Most importantly, the similar statin-like behaviour, exhibited by BMF treated rats, represents an important scientific evidence supporting the already known hypolipidemic effects of diet integration with some citrus species, among them bergamot. In our experimental model, the increase in HMGR, LDLR and FASN expression under BMF treatment is clearly evident and, to our knowledge, these results have been reported here for the first time. Taken together, these latter outcomes are in accord with the hypolipidemic effects observed in rat blood indeed, the decrease of TC and LDL concentrations is likely due to a blockade of HMGR activity and to an induced expression of hepatic LDLR. As it is known, HMGR expression and activity may change in response to the content of local cholesterol in cells and/or tissues. In this case, HMGR inhibition by the drugs used in our model lead to a reduction of endogenous cholesterol, which, in turn, is responsible of the upregulation of HMGR and LDLR gene transcriptions, as well of a higher LDLR exposure within the hepatocytes membrane likely through a compensating mechanism probably based on SREBPs pathway as already reported. Most likely, in our model the depletion of cholesterol below a certain threshold is also responsible of the increase of FASN gene transcription elicited by both simvastatin and BMF in rat, via SREBPs activation. Summing up, as depicted in figures 15-17, the daily supplementation with BMF is able to significantly reduce TC, TG and LDL levels in a similar extent to simvastatin treatment and more important, contemporaneously to increase HDL blood levels. These data establish, in a model that is highly relevant to humans, that inhibition effectuated by BMF on HMGR is a promising therapeutic strategy to raise plasma HDL and to low LDL levels for the treatment of hypercolesterolemia that increase cardiovascular disease risk.

Beside the rat model the yeast model was used to express the protein HMGR and evaluate the response of sterol metabolism in *S. cerevisiae* after treatment with pravastatin and BMF.

In our yeast system, we confirm the up-regulation of HMGR mRNA after statin and BMF treatments. In an attempt to mask the less enzyme activity, the cell increases the production of mRNA to restore the physiological levels of the protein. The inhibition of the regulatory enzyme, paradoxically stimulates its own production and cause the slowing of flow through the corresponding pathway.

Pravastatin and BMF treatments both induced expression of wild-type human HMGR gene. This is in accordance with other studies, which showed increased expression of the human HMGR gene in HepG2 and L cells, as well as in human skeletal muscle-like cells following statin treatment [98, 99]. We postulate that inhibition of HMGR activity trough BMF treatment may trigger an adaptive response in the cell.

In contrast to the up-regulation of HMGR gene, both the pravastatin and BMF lowered the total sterols. These results have showed that BMF cause a multiple actions i.e. beyond the direct inhibition of HMGR enzyme it is involved in modulation of cell lipid metabolism by lowering the sterol content.

Finally, the bacterial model chosen as in vitro system, allowed the successful expression of recombinant cf-HMGR in the *E.coli* cells. Although a significant fraction of the protein precipitates in the form of IB, the small fraction found in the cytosol, has been sufficient for subsequent investigations eliminating the problem of solubilization and renaturation that often strongly reduces the possibilities of kinetic study and characterization of heterologous proteins expressed in bacteria systems.

Mevalonic acid production was optimal between pH 6.5 and 7.5, with an optimum activity at pH 6.8 (Fig. 23). In the inhibition studies, the pravastatin competes with the HMG-CoA substrate, for binding to the active site of the enzyme. With increasing concentration of pravastatin, we observed a reduction of absorbance dose-dependent (Fig. 24). Furthermore the cytosolic fraction containing the expressed protein was used to investigate the activity of BMF on cf-HMGR. The catalityc activity of cf-HMGR is influenced by low concentration of BMF. As shown in figure 26, at 25 uM was obtained a reduction of catalytic activity near to 45%. We can claim to have achieved the catalytic portion of the enzyme in soluble and active form and that we have set the best conditions for the spectrophotometric assay.

With the goal to obtain a system not influenced by external factors we purified the cf-HMGR. Since the activity of the protein after purification is lower than that measured for the cytosolic fraction (retains about 68% of the activity) it was necessary a process of renaturation. This procedure conducted in a reducing buffer was time dependent and has allowed the full recovery of the activity. In conclusion we can claim to have a system that can be used in order to make a screening of different substances with alleged hypocholesterolemic activity.

CONCLUSION

The hypocholesterolemic activity of BMF has been evaluated by study conducted in vivo and in vitro.

The data obtained from in vivo assay establish, in a model that is highly relevant to humans, that inhibition effectuated by BMF on HMGR is a promising therapeutic strategy to raise plasma HDL and to low LDL levels for the treatment of hypercholesterolemia that increase cardiovascular disease risk. Furthermore it has been demonstrated that BMF could have multiple effects acting directly on HMGR enzyme and indirectly on the cell lipid metabolism.

The data obtained with in vitro system confirm the inhibitor capacity of BMF and offer a valid tool for the rapid and easy screening of different substances with alleged hypocholesterolemic activity.

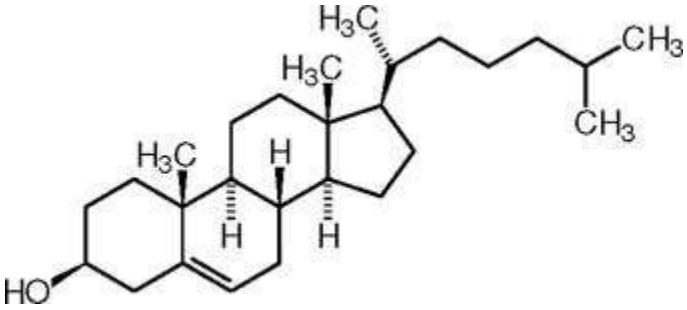

Figure 1: Cholesterol structure

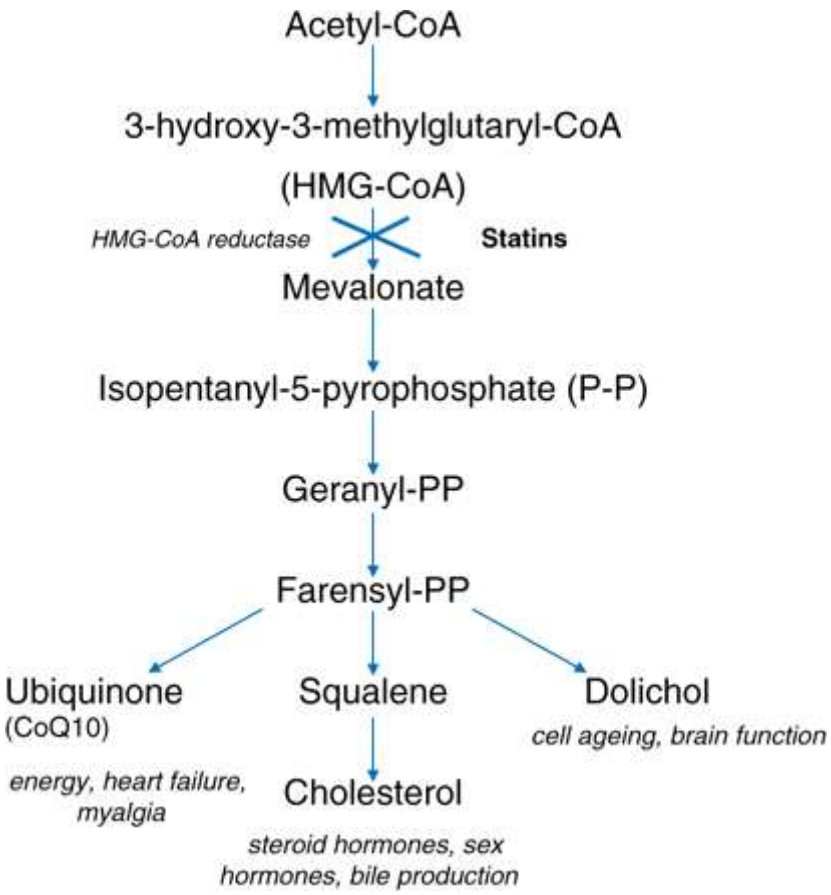

Figure 2: Mevalonate pathway

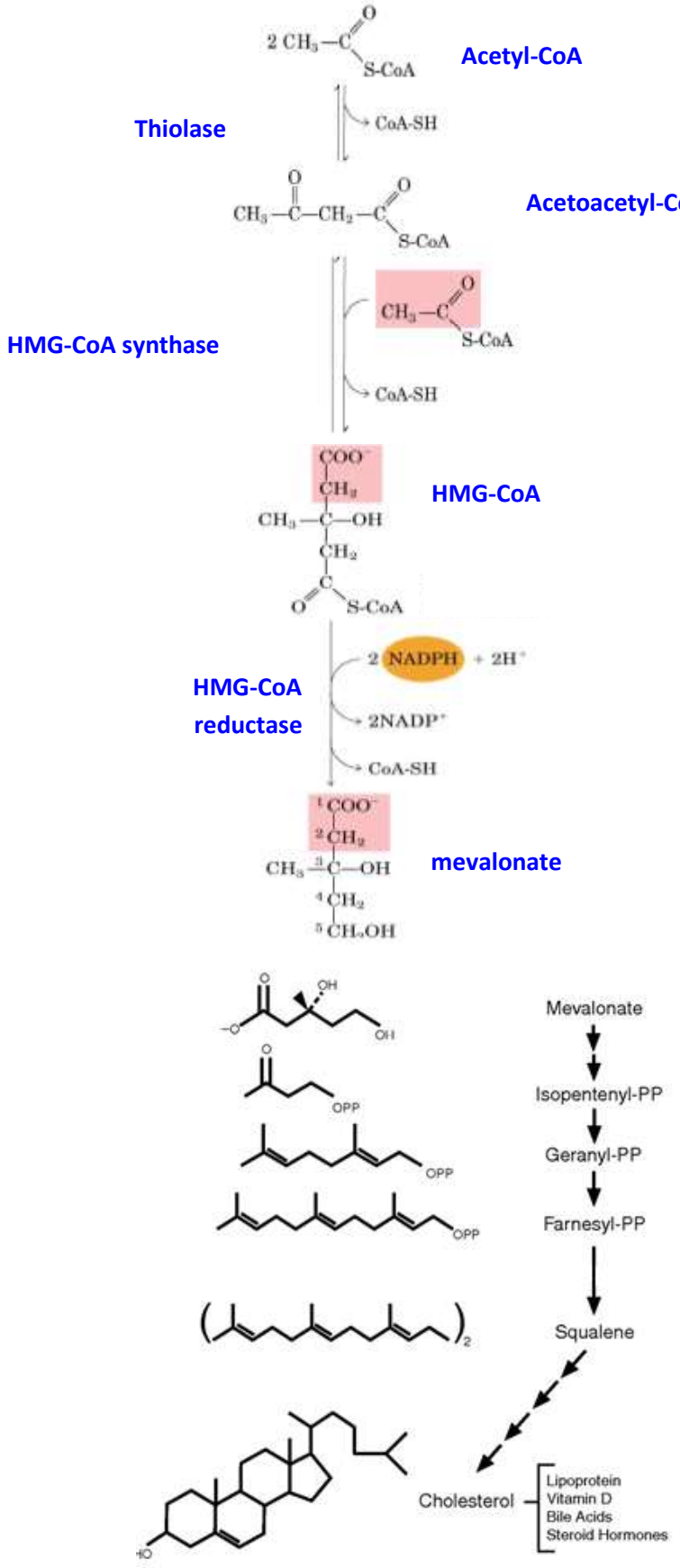

Figure 3: Cholesterol synthesis

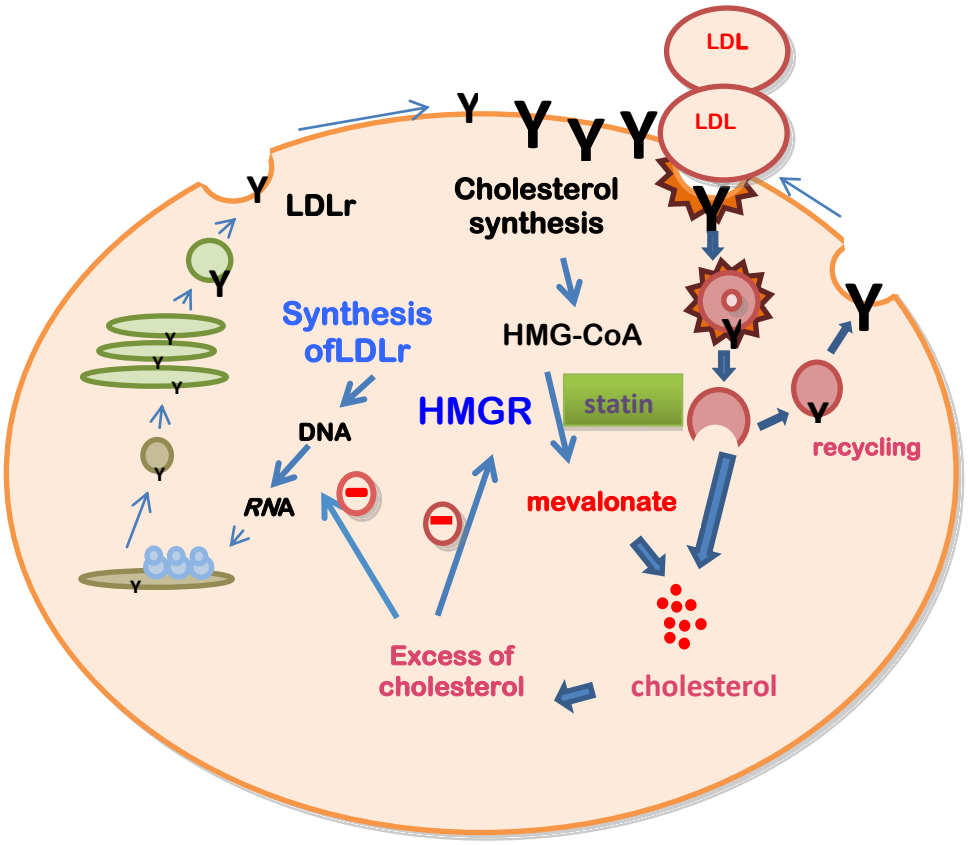

Figure 4: Cholesterol homeostasis

The cholesterol enters in hepatocytes as LDL through a receptor mediated endocytosis .

The cholesterol homeostasis is ensured through several mechanisms.

- Block HMGR enzyme by excess of cholesterol in the cell.
- Inhibition of transcription of the genes involved in the synthesis of the LDL receptor (LDLr).

Statins block the HMGR enzyme involved in mevalonate synthesis.

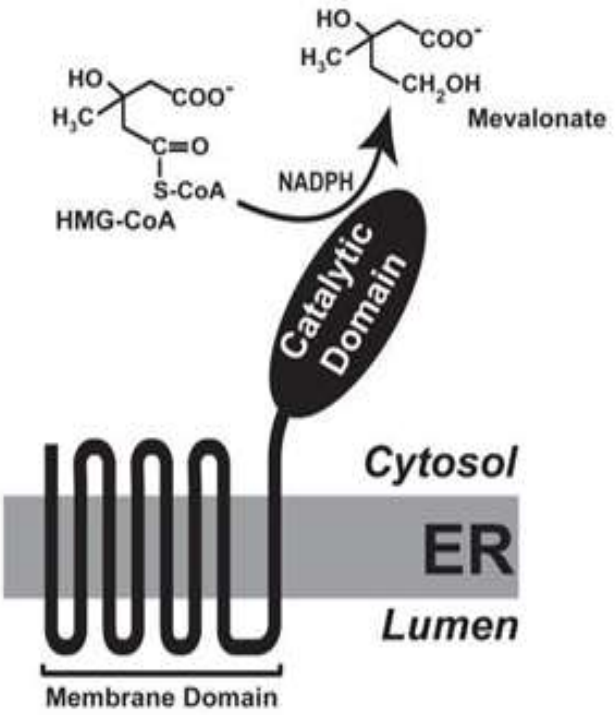

Figure 5: Human HMGR structure

Human HMGR is an integral glycoprotein of the endoplasmic reticulum. The protein consists of a single polypeptide chain of 97-kDa.
HMG CoA reductase consists of two distinct domains: a hydrophobic N-terminal domain with eight membrane-spanning segments that anchor the protein to endoplasmic reticulm (ER), and a hydrophilic C-terminal domain that projects into the cytosol and exhibits all of the enzyme's catalytic activity.

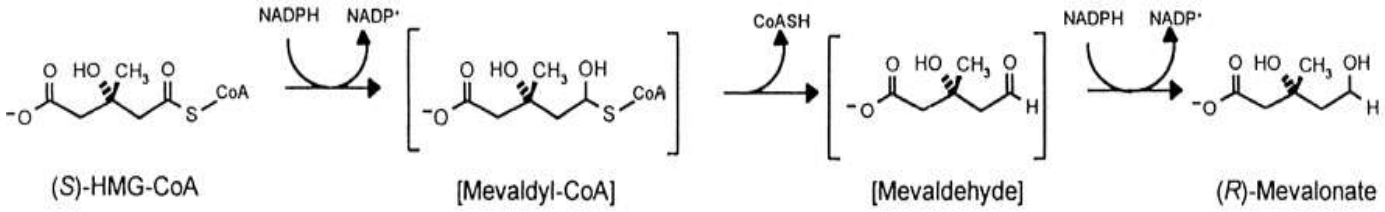

Figure 6: Reaction of HMGR

HMGR, catalyzes conversion of HMG-CoA to mevalonate, the precursor of isoprenoid groups. Catalysis by this 4-electron oxidoreductase proceeds in three stages, the first and third of which are reductive.

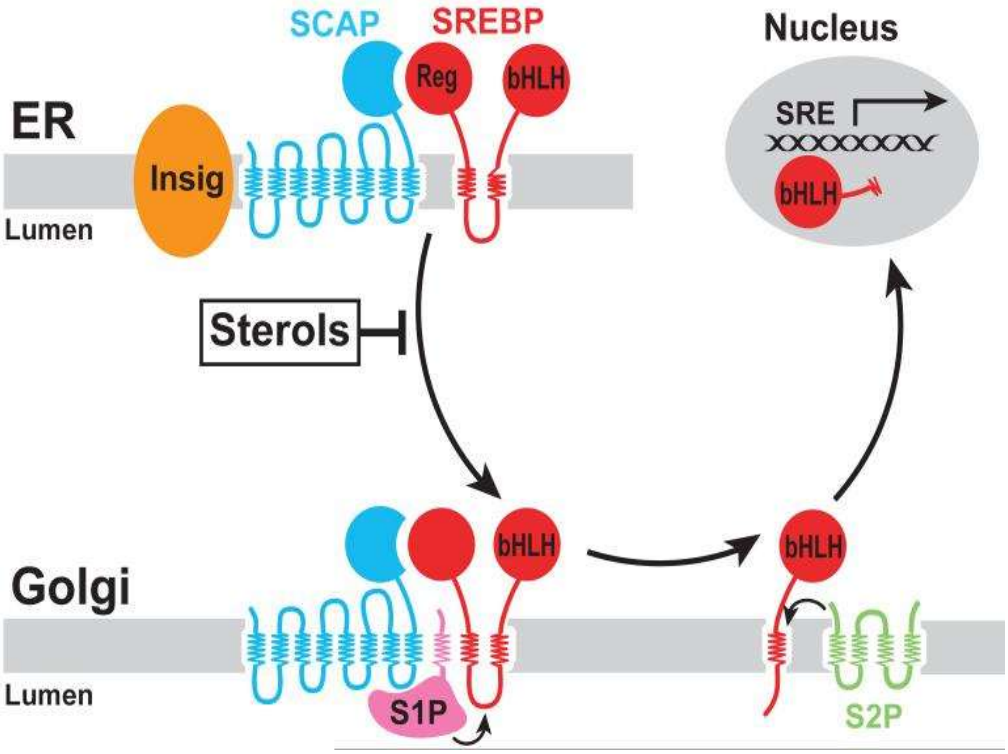

Figure 7: Regulation of HMRG by SREBP

Model for sterol-regulated Scap-SREBP pathway. SCAP is a sensor of sterols and an escort of SREBPs. In sterol-depleted cells, Scap facilitates export of SREBPs from the ER to the Golgi apparatus, where two proteases, Site-1 protease (S1P) and Site-2 protease (S2P), act to release the transcriptionally active, N-terminal basic-helix-loop-helix-leucine-zipper (bHLH-Zip) domain of SREBPs from the membrane. The released bHLH-Zip domain migrates into the nucleus and binds to a sterol response element (SRE) in the enhancer/promoter region of target genes, activating their transcription. Accumulation of sterols in ER membranes triggers binding of Scap to one of two retention proteins called Insigs, which blocks incorporation of Scap-SREBP complexes into ER transport vesicles. As a result, SREBPs no longer translocate to the Golgi apparatus, the bHLH-Zip domain cannot be released from the membrane, and transcription of all target genes declines.

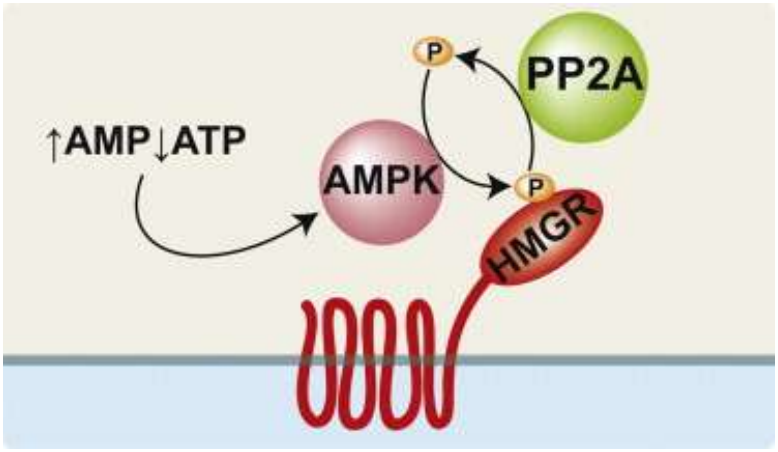

Figure 8: Regulation of HMRG by AMPK

Mammalian HMGR catalytic activity is regulated by AMP kinase. A high AMP:ATP ratio stimulates AMP-activated protein kinase (AMPK), which phosphorylates HMGR at a conserved serine in the active site, thus inhibiting HMGR activity. Protein phosphatase 2A (PP2A) dephosphorylates HMGR, restoring enzyme activity.

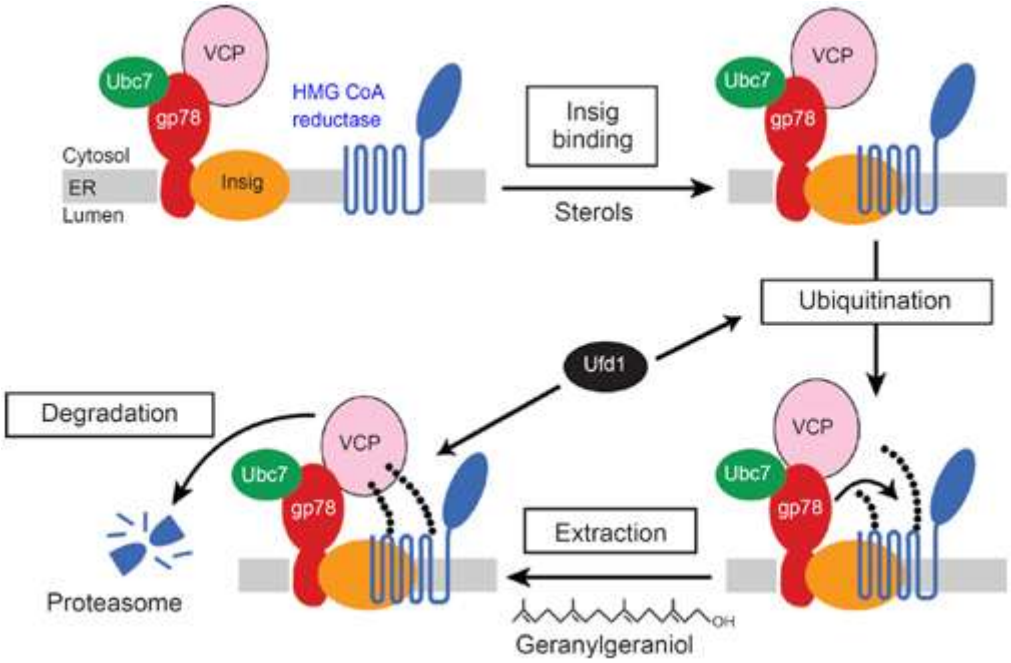

Figure 9: Regulation of HMRG by degradation

Pathway for sterol-accelerated degradation of HMG CoA reductase. Accumulation of 25-hydroxycholesterol, lanosterol, or 24,25-dihydrolanosterol in ER membranes triggers binding of the reductase to Insigs. A subset of Insigs is associated with the membrane-anchored ubiquitin ligase, gp78, which binds the E2 Ubc7 and VCP, an ATPase that plays a role in extraction of ubiquitinated proteins from ER membranes. Through the action of gp78 and Ubc7, reductase becomes ubiquitinated, which triggers its extraction from the membrane by VCP, and subsequent delivery to proteasomes for degradation. The post-ubiquitination step is postulated to be enhanced by geranylgeraniol through an undefined mechanism that may involve a geranylgeranylated protein, such as one of the Rab proteins.

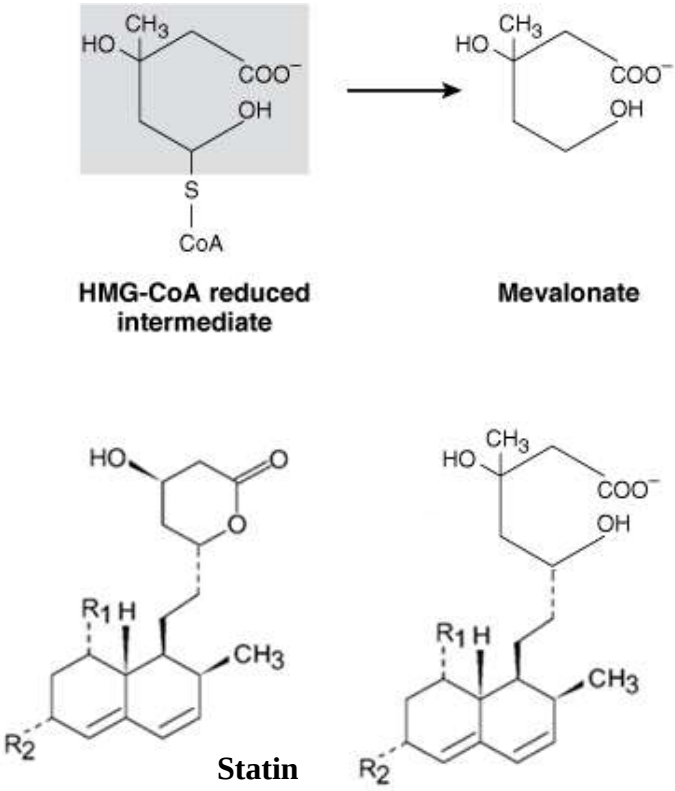

Figure 10: Statin structure

In the figure is shown the similarity between the active nucleus of statins and the HMG-CoA structure.

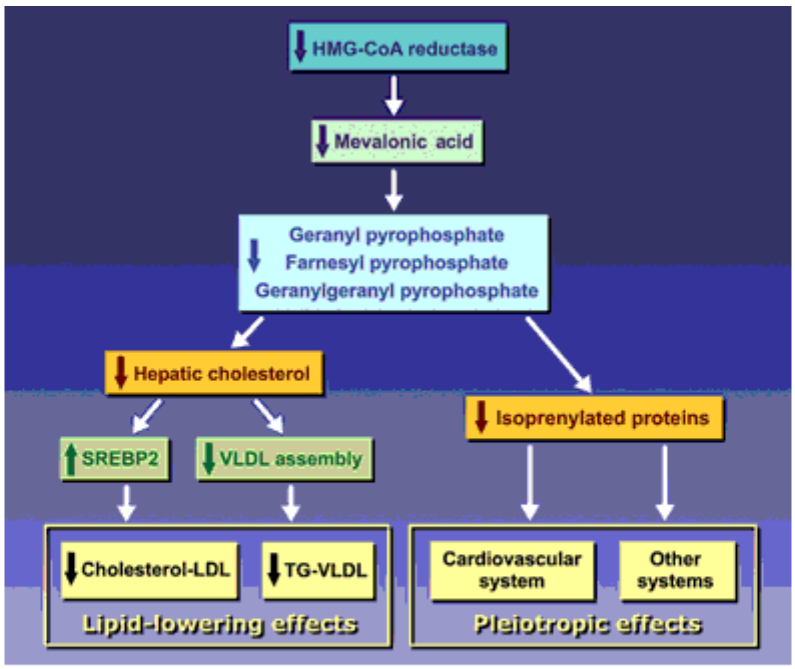

Fig. 11: Statins effects

In the figure are summarized the numerous effects of statins treatment.

A

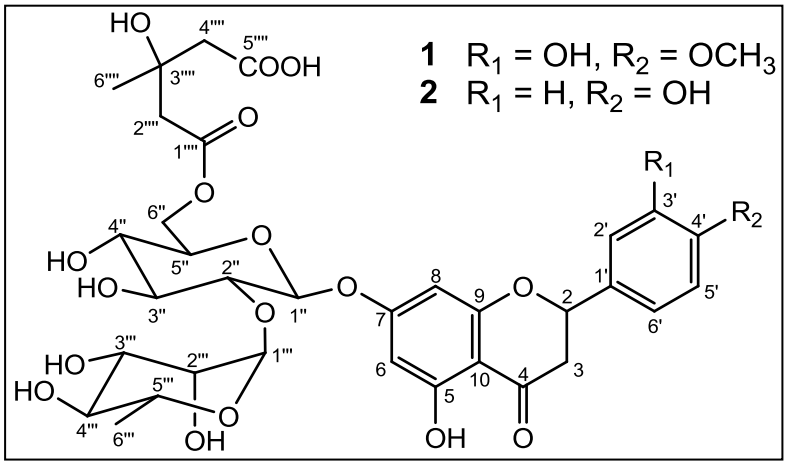

B

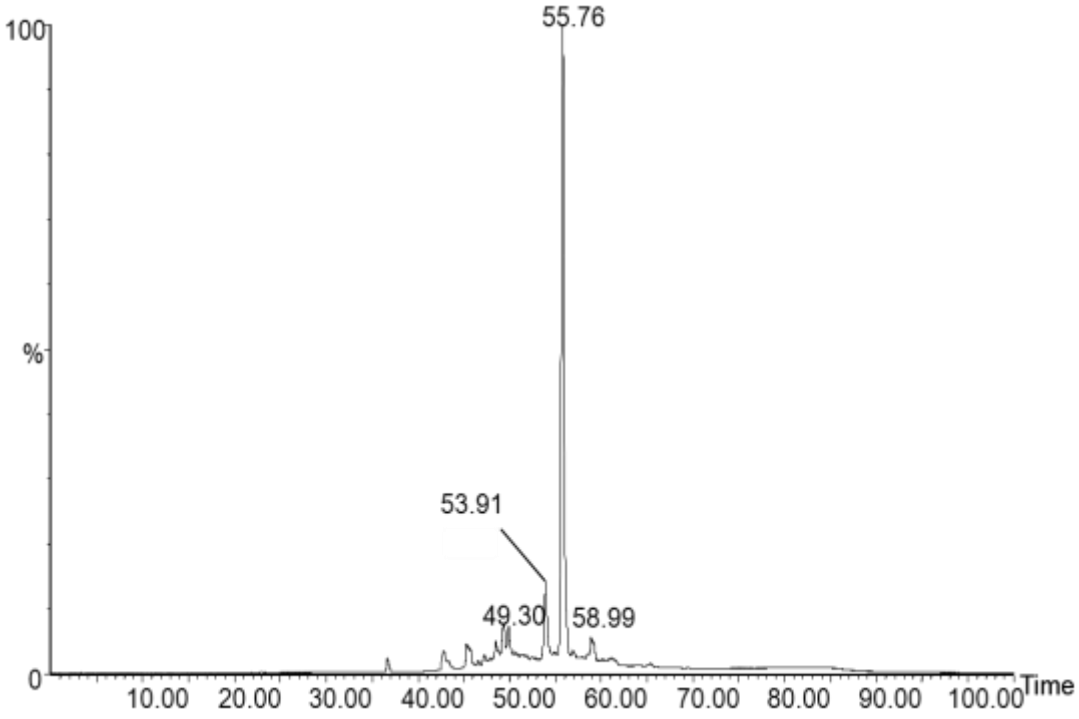

Figure 12: A: 1 brutieridin ; 2 melitidin structures
B: HPLC / UV 280 nm of brutieridin (1, rt 55,76) and melitidin (2, rt 53,91) enriched fraction (BMF)

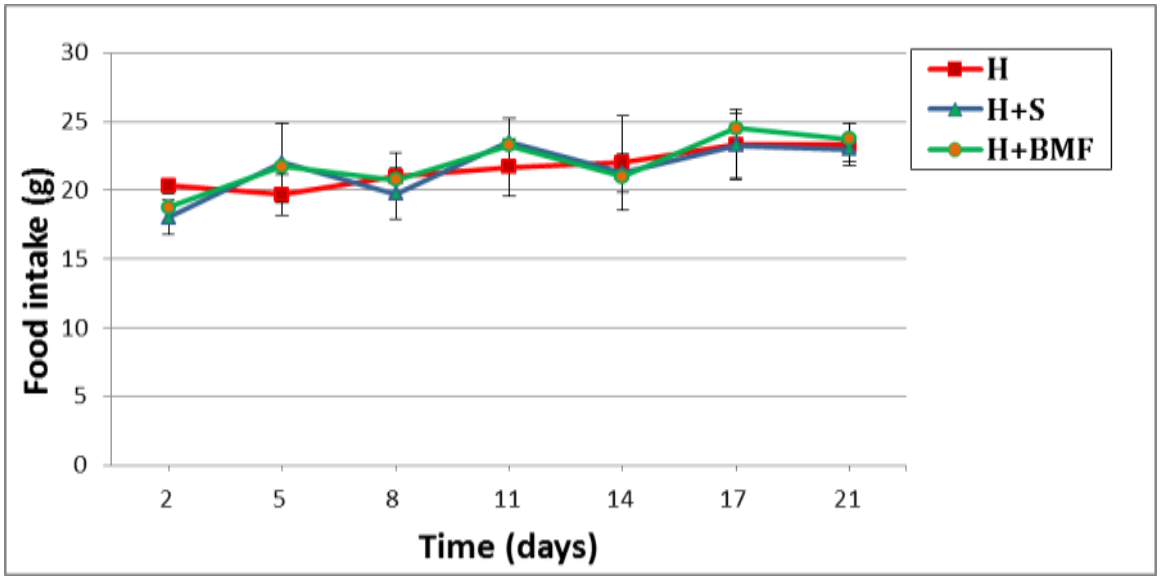

Figure 13: Summary of daily food intake respect to the entire experiment period for each group of rats. Hypercholesterolemic rats group (red squares, H) were fed on a 5% enriched cholesterol diet and used as control in these experiments, the hypercholesterolemic groups were treated with simvastatin (20 mg/kg bw/day; green triangles, H+S) and with BMF (60 mg/kg bw/day; orange circles, H+BMF), starting from the end of the 1st week. Values represent the mean ± SD of the daily chow intake for each rat in respect to the group.

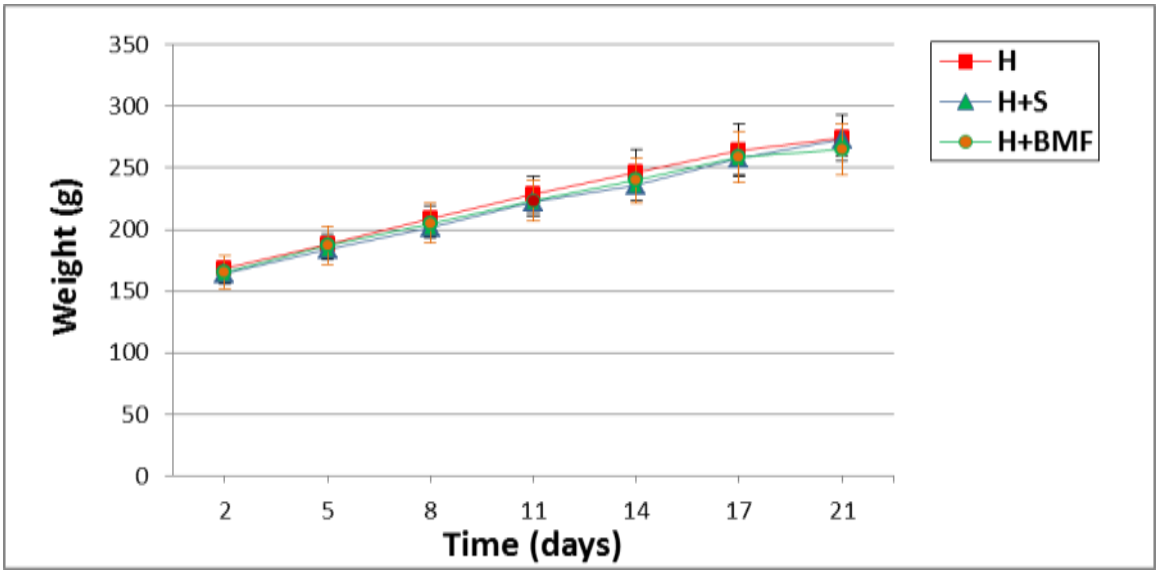

Figure 14: Summary of body weight changes over the study period for each group of rats. Hypercholesterolemic rats group (red squares, H) were fed on a 5% enriched cholesterol diet and used as control in these experiments, the hypercholesterolemic groups were treated with simvastatin (20 mg/kg bw/day; green triangles, H+S) and with BMF (60 mg/kg bw/day;orange stars, H+BMF), starting from the end of the 1st week. Values represent the mean ± SD of the daily weight for each rat in respect to the group.

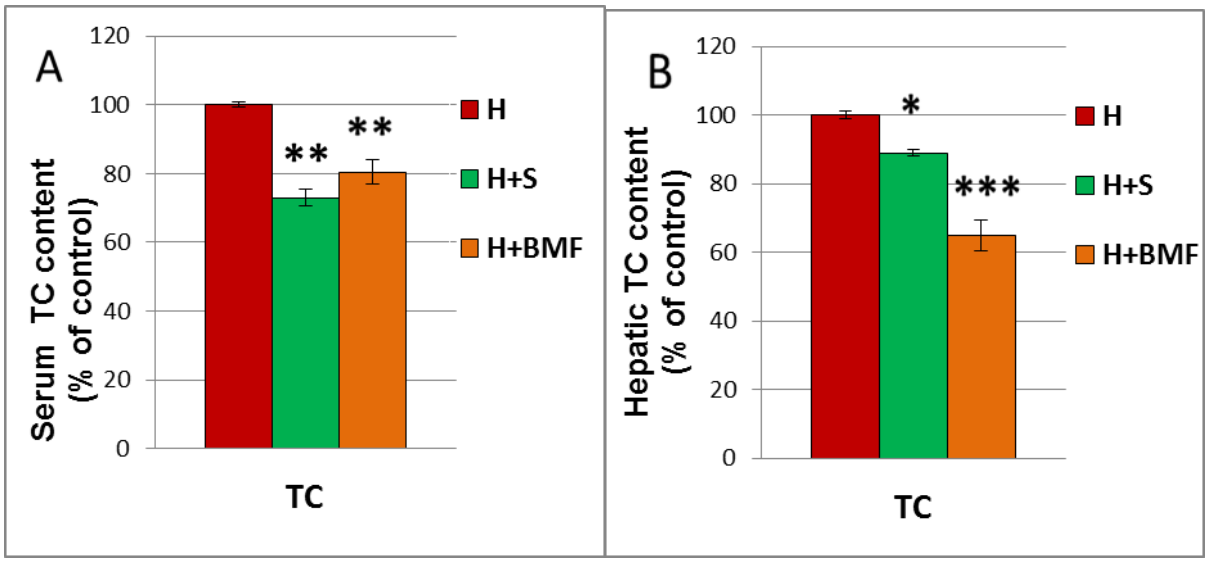

Figure 15 : Effects of simvastatin and BMF administration on serum and hepatic total cholesterol (TC).Hypercholesterolemic rats group (red bars, H) were fed on a 5% enriched cholesterol diet and used as control in these experiments, the hypercholesterolemic groups were treated with simvastatin (20 mg/kg bw/day; green bars, H+S) and with BMF (60 mg/kg bw/day; orange bars, H+BMF), starting from the end of the 1st week. TC levels were measured in serum (A) and liver (B), the results obtained were plotted as percentage respect to the H group (which was on average 80 mg/dl and 3.4 mg/g liver, respectively). Columns are mean ± SD of 3 independent experiments performed in duplicate. The experiments are representative of at least 3 separated assays. *, P = 0.01 vs. control; **, P < 0.01 vs. control; ***, P < 0.005 vs. control.

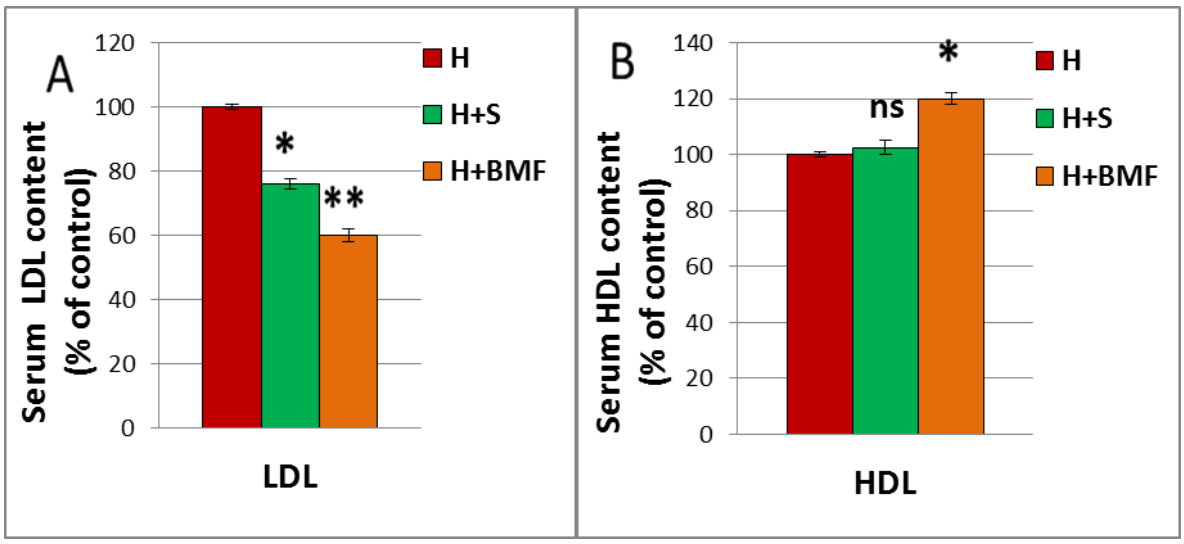

Figure 16 : Effects of simvastatin and BMF administration on serum LDL and HDL. Hypercholesterolemic rats group (red bars, H) were fed on a 5% enriched cholesterol diet and used as control in these experiments, the hypercholesterolemic groups were treated with simvastatin (20 mg/kg bw/day; green bars, H+S) and with BMF (60 mg/kg bw/day; orange bars, H+BMF), starting from the end of the 1st week. Serum LDL (A) and HDL (B) levels were measured and plotted as percentage in respect to H group (which was on average 42 mg/dl and 34 mg/dl, respectively). Columns are mean ± SD of 3 independent experiments performed in duplicate. ns, nonsignificant; *, $P < 0.01$ vs. control; **, $P < 0.005$ vs. control.

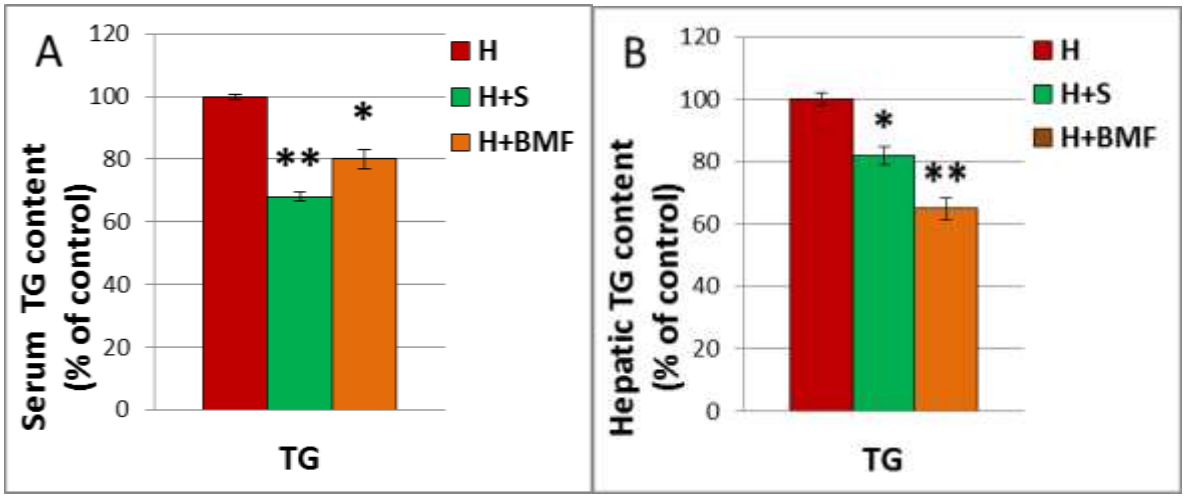

Figure 17 :Effects of simvastatin and BMF administration on serum and hepatic triglycerides (TG). Hypercholesterolemic rats group (red bars, H) were fed on a 5% enriched cholesterol diet and used as control in these experiments, the hypercholesterolemic groups were treated with simvastatin (20 mg/kg bw/day; green bars, H+S) and with BMF (60 mg/kg bw/day; orange bars, H+BMF), starting from the end of the 1st week. TG levels were measured in serum (A) and liver (B), the obtained results were plotted as percentage in respect to the H group (which was on average 105 mg/dl and 7 mg/g liver, respectively). Columns are mean ± SD of 3 independent experiments performed in duplicate. The experiments are representative of at least 3 separated assays. *, $P < 0.01$ vs. control; **, $P < 0.005$ vs. control.

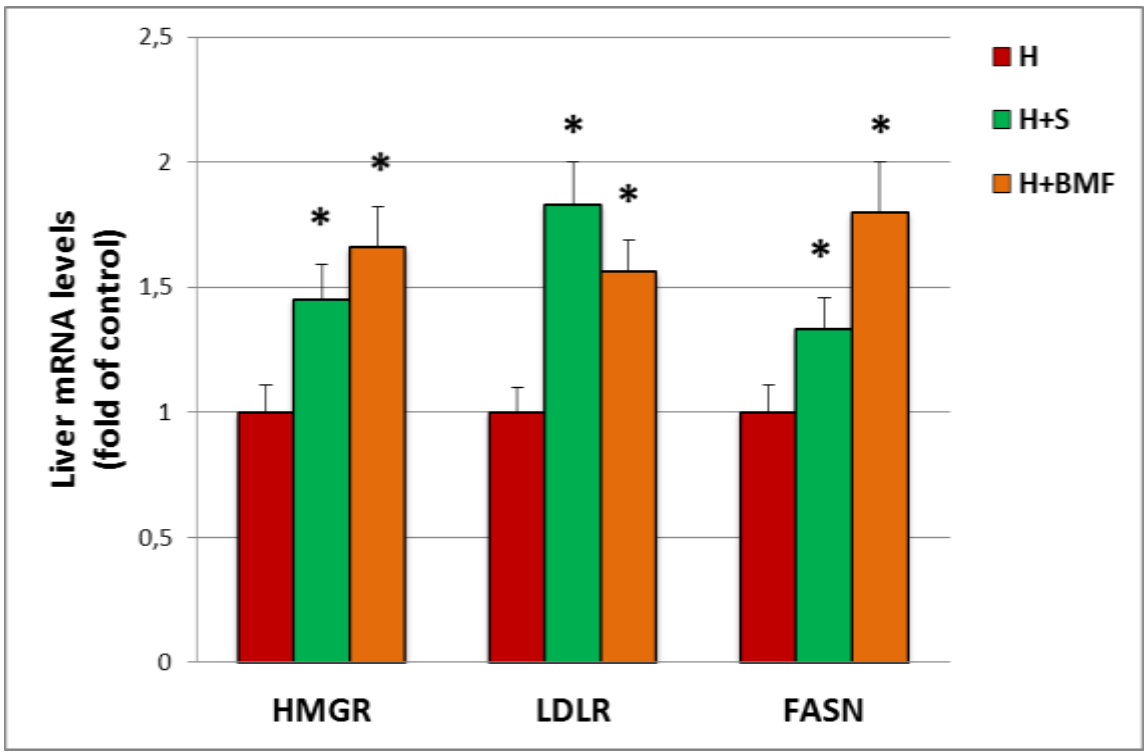

Figure 18 : Up-regulation of liver HMGR, LDLR and FANS mRNA expression levels by administration of simvastatin and BMF in experimental rats. Livers were isolated from hypercholesterolemic untreated rats (red bars, H), hypercholesterolemic rats treated with simvastatin (green bars, H+S) or with BMF (orange bars, H+BMF). HMGR, LDLR and FASN mRNA levels were analyzed by RT-PCR and normalized to that of 18S. The values were plotted as fold of untreated hypercholesterolemic group which was designated as H. Values are mean ± SD of all of the animals in each group and are representative of 3 independent experiments. *, $P < 0.01$ vs.
control.

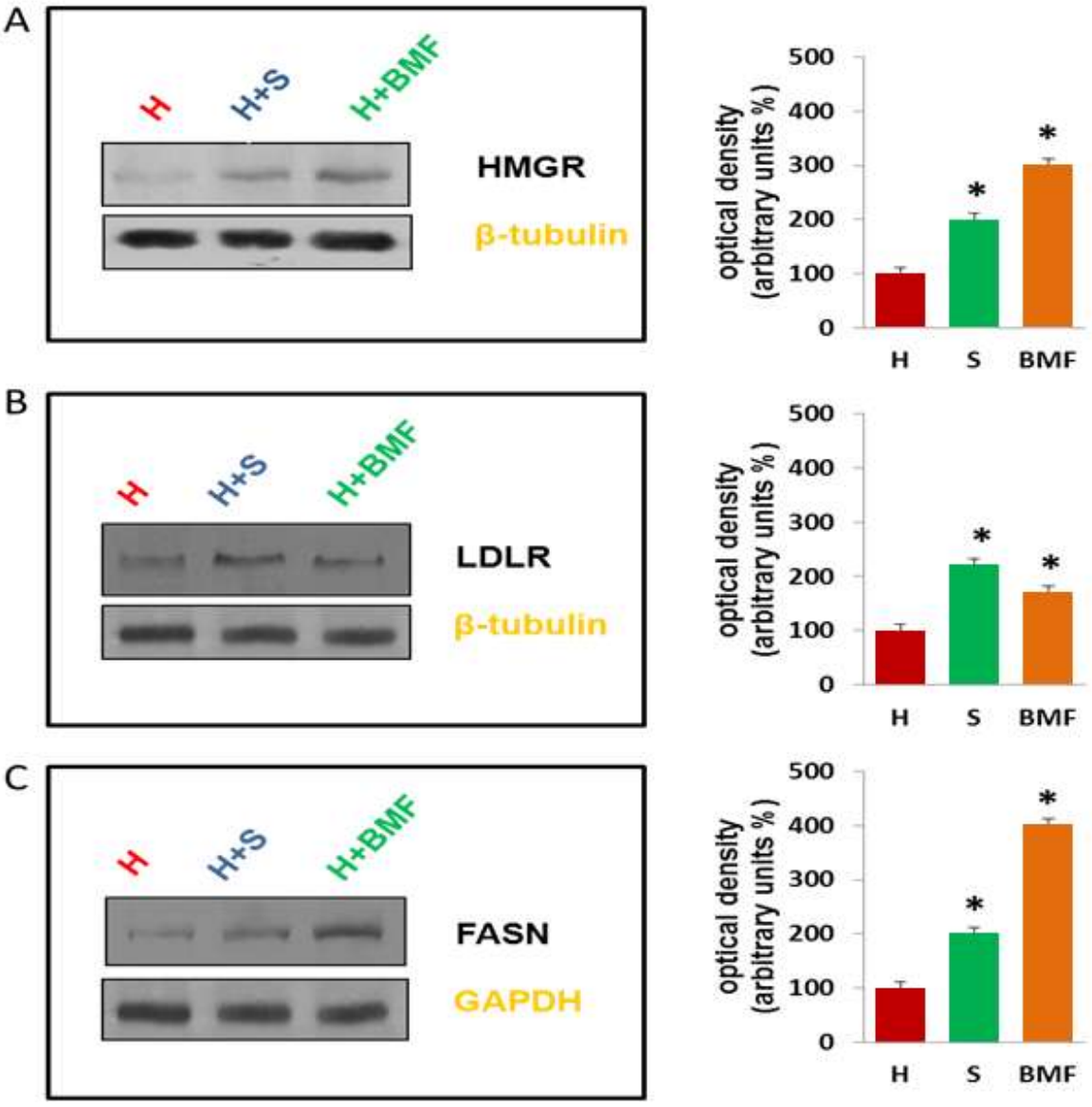

Figure 19 : Effect of simvastatin and BMF on HMGR, LDLR and FASN proteins expression in experimental rats. The figure shows proteic levels of (A) HMGR (97 kDa), (B) LDLR (160 kDa) and (C) FASN (270 kDa). A total of 100 µg of microsomes or cellular liver extract were used for Western blot analysis of hypercholesterolemic 21 untreated rats (H), or hypercholesterolemic treated rats with simvastatin (H+S) or
BMF (H+BMF). ß-tubulin (55 kDa) or GAPDH (37 kDa) were used as a control for equal loading and transfer. The immunoblots shown are representative of 3 separate experiments. Side panels show densitometric analysis of the blots. *, $P < 0.01$ vs. control.

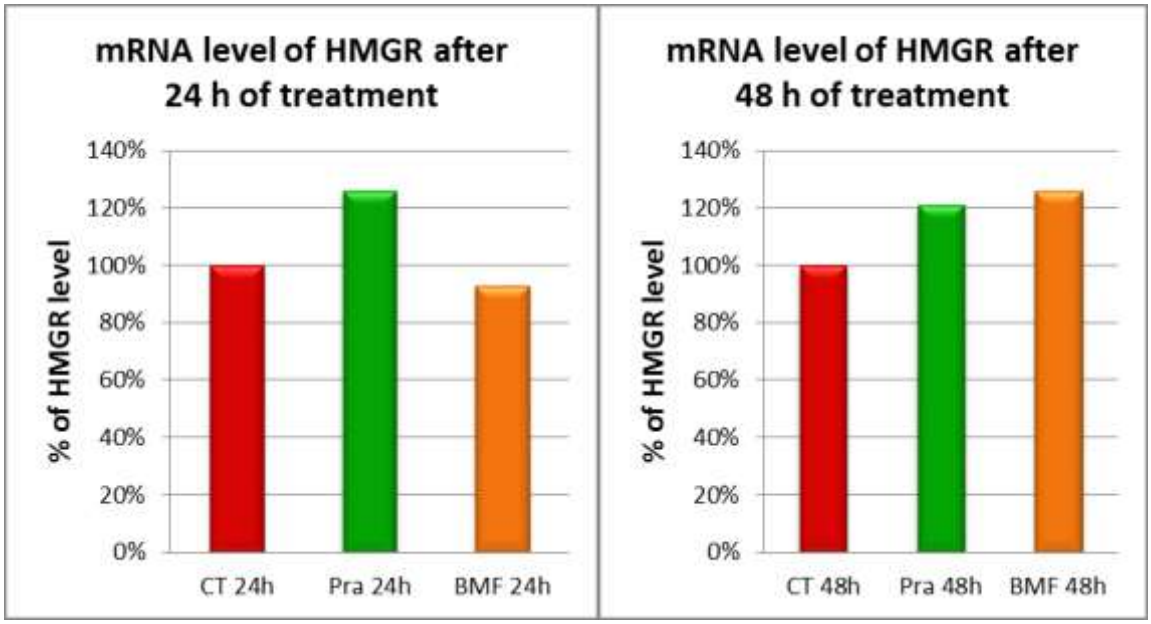

Figure 20 : Up-regulation of HMGR mRNA expression levels by administration of pravastatin and BMF in yeast. Untreated cells (red bars; control CT), cells treated with pravastatin (gren bars; Pra) or with BMF (orange bars). HMGR mRNA levels were analyzed by RT-PCR and normalized to that of 35S. The values were plotted as percent respect to untreated cells. Values are representative of 3 independent experiments.

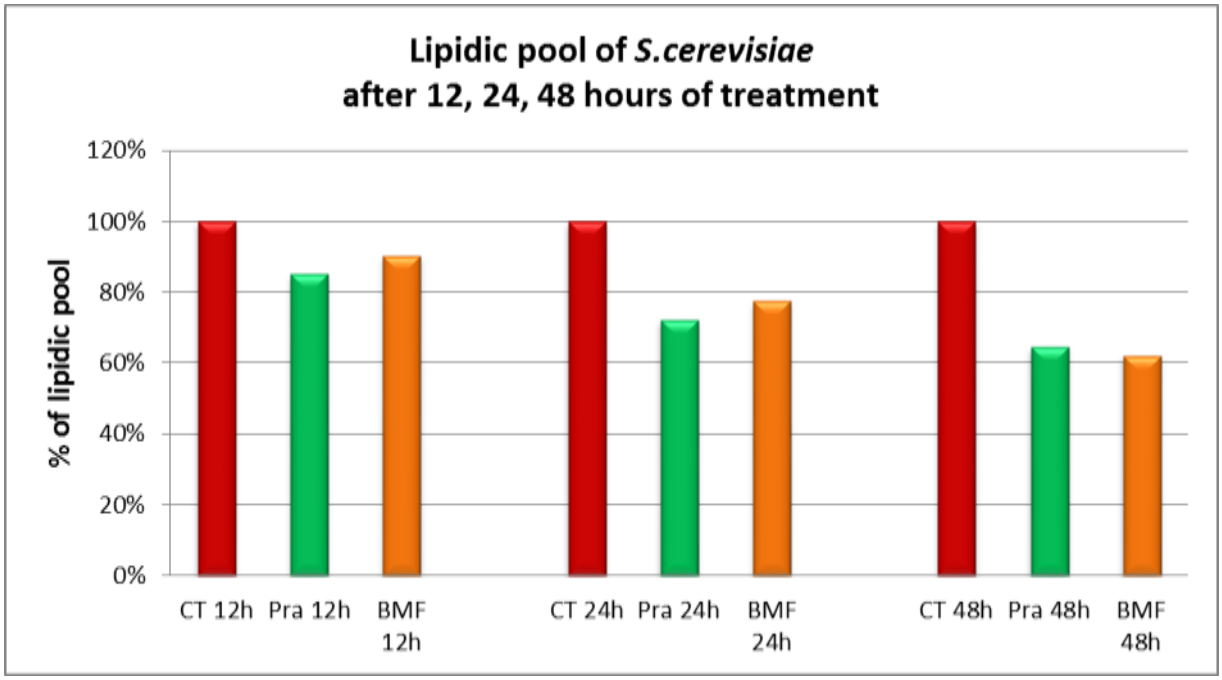

Figure 21: Down-regulation of sterol pool expression levels by administration of pravastatin and BMF in yeast. Untreated cells (red , bars; control CT), cells treated with pravastatin (gren bars; Pra) or with BMF (orange bars). Sterol levels were analyzed by HPLC/UV. The values were plotted as percentage of sterol content in untreated cells. Values are representative of 3 independent experiments.

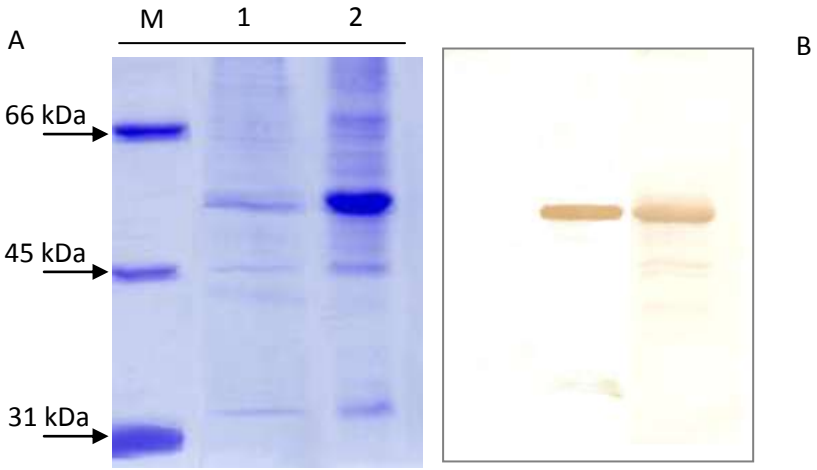

Figure 22

A: Expression gel

In the lane 1 was loaded the cytosolic fraction and in the lane 2 was loaded the IB from *E. coli* coding for recombinant plasmid cf-HMGR

B: Western-blot of cytosolic fraction and IB from *E. coli* coding recombinant plasmid cf-HMGR**.**

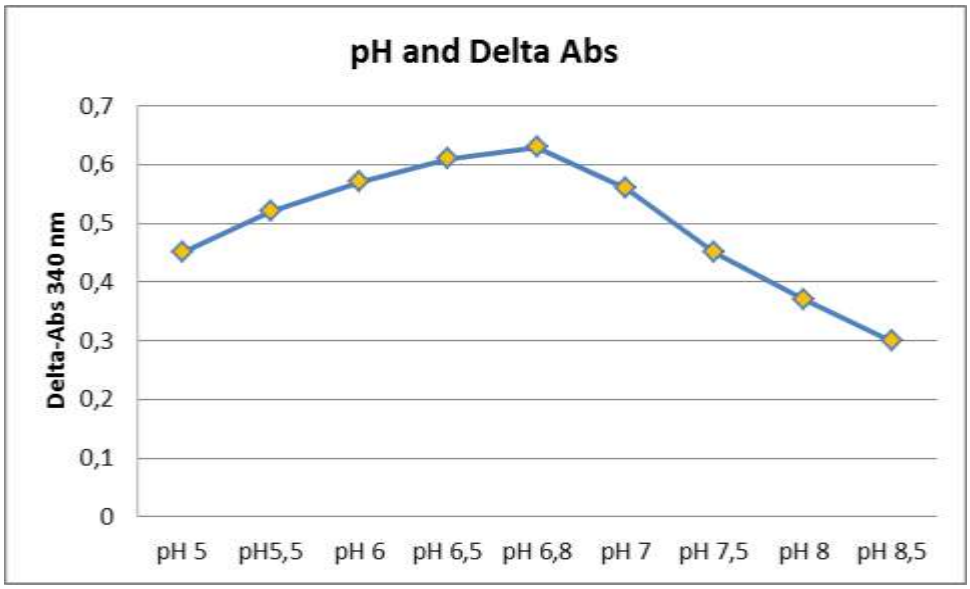

Figure 23 : pH dependent-enzymatic activity

Variation of absorbance at 340 nm depends upon the pH values. Mevalonic acid production is optimal between pH6.5 and 7.5, with an optimum activity at pH 6.8. The cf-HMGR activity decreasing rapidly below pH6.0 and above pH 8.0

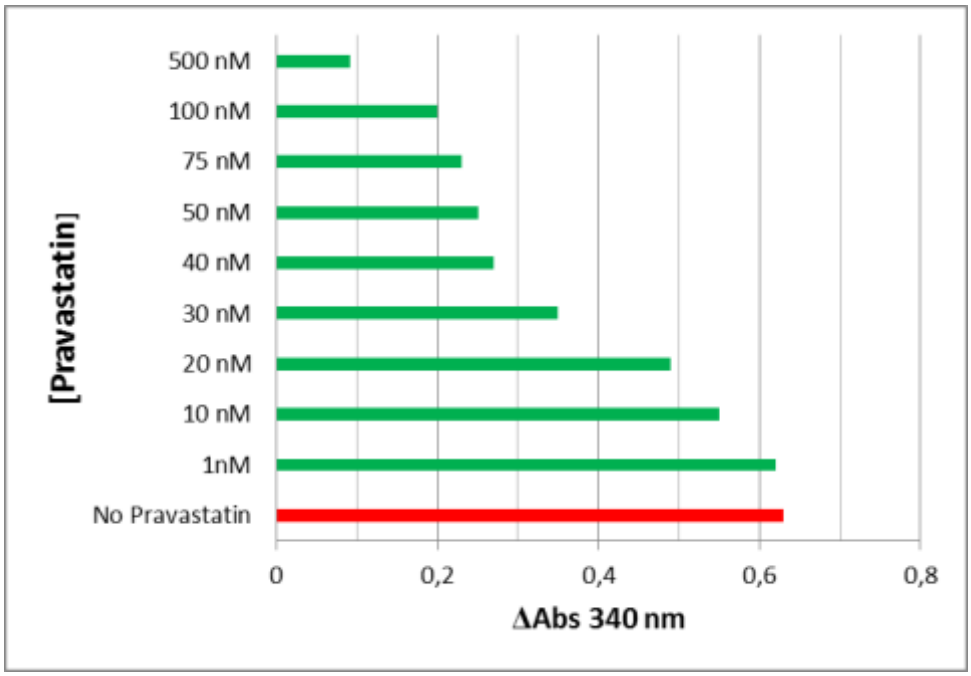

Figure 24 : Percentage of HMGR activity inhibition

The pravastatin competes with the HMG-CoA substrate, for binding to the active site of the enzyme. In the figure is shown the variation of the absorbance at 340 nm upon the concentration of pravastatin.

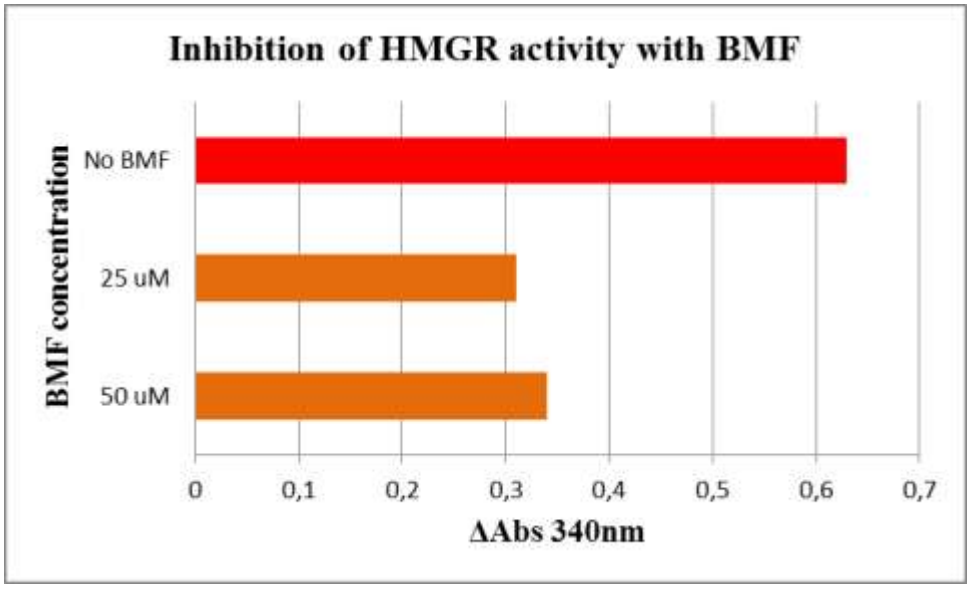

Figure 25 : Inhibition of HMGR activity with BMF

The BMF competes with the HMG-CoA substrate, for binding to the active site of the enzyme. In the figure is shown the variation of the absorbance at 340 nm upon the concentration of BMF.

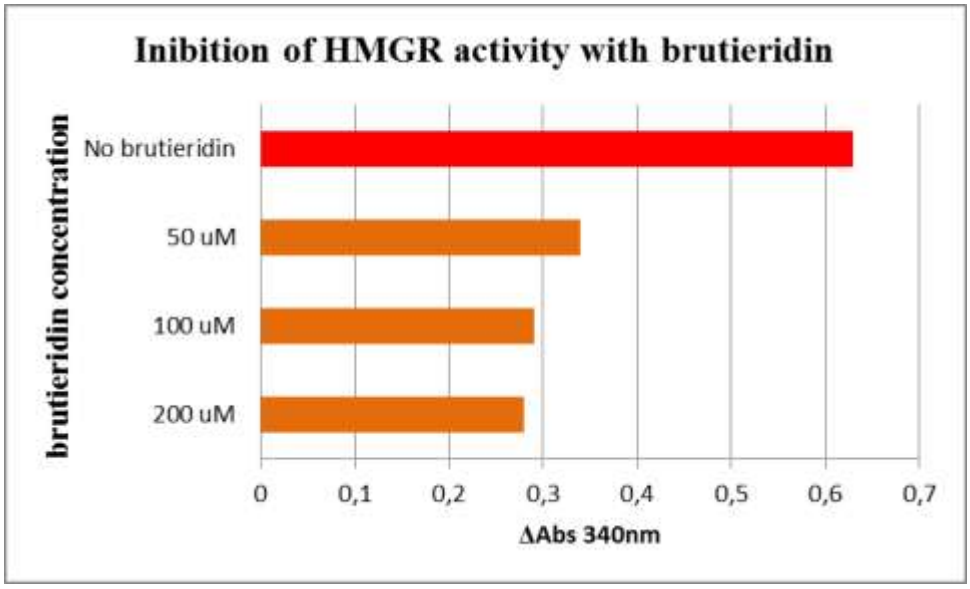

Figure 26 : Inhibition of HMGR activity with brutieridin

The brutieridin competes with the HMG-CoA substrate, for binding to the active site of the enzyme. In the figure is shown the variation of the absorbance at 340 nm upon the concentration of brutieridin.

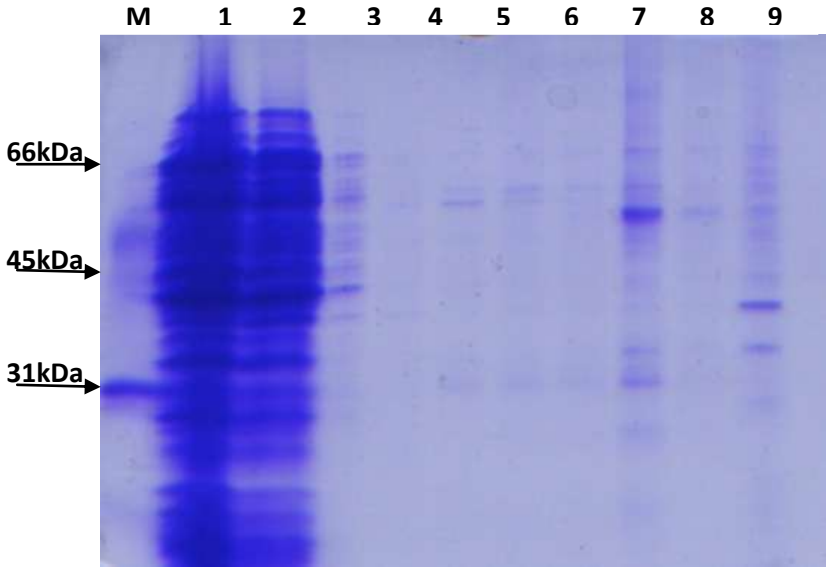

Figure 27 : **Purification Gel.**

Lane M: molecular weight marker; Lane 1: first eluated; Lanes 2-6: washing with imidazole from 5 mM to 40 mM; Lanes 7-9 eluated with imidazole 80 mM; Lane 10 washing with 10% SDS.

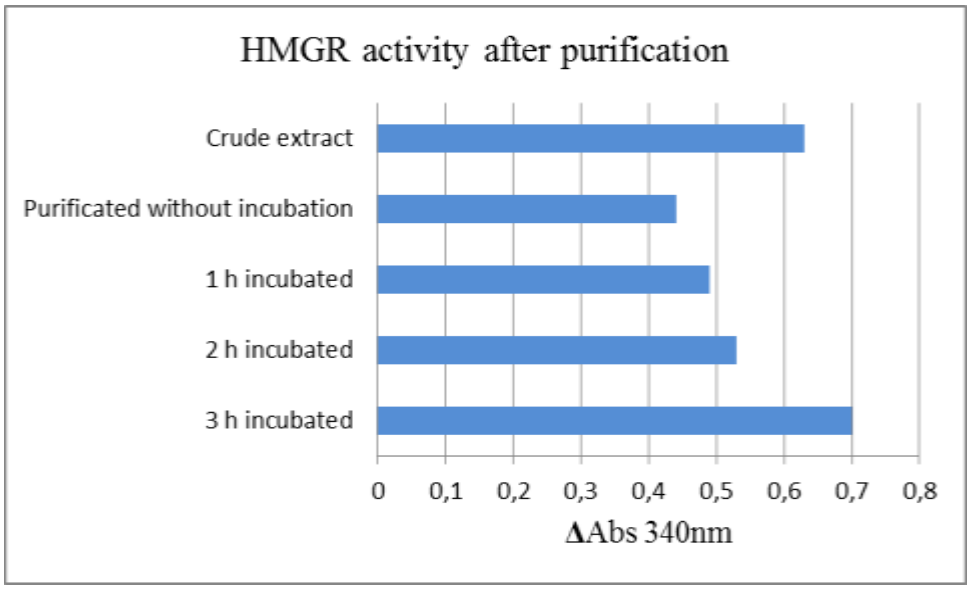

Figure 28 : HMGR activity after purification

Variation of absorbance at 340 nm after the renaturation procedure. Three hours of incubation in buffer assay reaches the full recovery of the activity.

Table 1

Oligonucleotides used for HMGR constructs

The cloning site are showed in bold

Construct	Oligo name	Oligonucleotide sequence
pETV5-His-HMGR	pETV5-His-HMGR For1	5'- ATCACATCTCCTGTAGTGACAC -3'
pETV5-His-HMGR	pETV5-His-HMGR Rev 1	5'- CAGTGATCACATTTATTCATCCTCCA -3'
pETV5-His-HMGR	pETV5-His-HMGR For2	5'TGA**CATATG**TCCTCCTTACTCGATACTTCATCAGTAC -3'
pETV5-His-HMGR	pETV5-His-HMGR Rev 2	5'- CTA**GGATCC**GAGGCTGTCTTCTTGGTGCAAG -3'

REFERENCES

1. Yeagle PL. Lipid regulation of cell membrane structure and function. FASEB J. 1989; 3:1833–42;

2. Podar K, Anderson KC. Caveolin-1 as a potential new therapeutic target in multiple myeloma. Cancer Lett. 2006;233:10–15;

3. Pasqualini JR. Enzymes involved in the formation and transformation of steroid hormones in the fetal and placental compartments. J Steroid Biochem Mol Biol. 2005;97:401–415;

4. Vance DE, Van den Bosch H. Cholesterol in the year 2000. Biochim Biophys Acta. 2000; 1529:1–8;

5. Brown, MS, Goldstein, JL. A receptor-mediated pathway for cholesterol homeostasis. Science 1986; 232:34;

6. Espenshade PJ, Hughes AL. Regulation of sterol synthesis in eukaryotes. Annu Rev Genet. 2007;41:401–427;

7. Goldstein JL, Brown MS. Regulation of the mevalonate pathway. Nature. 1990;343:425–430;

8. Tolleshaug H, Hobgood KK, Brown MS, Goldstein JL. The LDL receptor locus in familial hypercholesterolemia: multiple mutations disrupt transport and processing of a membrane receptor. Cell. 1983;32:941–95;

9. Bays HE, Neff D, Tomassini JE, Tershakovec AM. Ezetimibe: cholesterol lowering and beyond. Expert Rev Cardiovasc Ther. 2008;6:447–470;

10. Ikonen E. Mechanisms for cellular cholesterol transport: defects and human disease. Physiol Rev. 2006;86:1237–1261;

11. Weber LW, Boll M, Stampfl A. Maintaining cholesterol homeostasis: sterol regulatory element-binding proteins. World J Gastroenterol. 2004;10:3081–3087;

12. Garber, AM, Avins, AL. Triglyceride concentration and coronary heart disease. Not yet proved of value as a screening test. BMJ 1994; 309:2;

13. Krause, RM, Williams, PT, Brensike, J, et al. IDL and progression of coronary disease in hypercholesterolemic men. Lancet 1987; 2:62;

14. Steinberg, D, Parthasarathy, S, Carew, TE, et al. Beyond cholesterol. Modifications of low-density lipoprotein that increase its atherogenicity. N Engl J Med 1989; 320:915;

15. Rosenson, RS, Tangney, CC. Elevated plasma viscosity contributes to CHD risk in subjects with hypertriglyceridemia. Circulation 1996; 94:1027;

16. Duverger, N, Kruth, H, Emmanuel, F, et al. Inhibition of atherosclerosis development in cholesterol-fed human apolipoprotein A-I-transgenic rabbits. Circulation 1996; 94:713;

17. C.Y. Yang, S.H. Chen, S.H. Gianturco, W.A. Bradley, J.T. Sparrow, M. Tanimura, W.H. Li, D.A. Sparrow, H. DeLoof, M. Rosseneu, Sequence, structure, receptor-binding domains and internal repeats of human apolipoprotein B-100, Nature, (1986), 323 pp. 738–742;

18. de Silva, HV, Lauer, SJ, Wang, J, et al. Overexpression of human apolipoprotein C-III intransgenic mice results in an accumulation of apolipoprotein B-48 remnants that is corrected by excess apolipoprotein E. J Biol Chem 1994; 269:2234;

19. Liscum L, Cummings RD, Anderson RG, DeMartino GN, Goldstein JL, Brown MS. 3-Hydroxy-3-methylglutaryl-CoA reductase: a transmembrane glycoprotein of the

endoplasmic reticulum with N-linked "high-mannose" oligosaccharides. Proc Natl Acad Sci U S A. 1983 Dec;80(23):7165–7169;

20. Brown MS, Dana SE, Dietschy JM, Siperstein MD. 3-Hydroxy-3-methylglutaryl coenzyme A reductase. Solubilization and purification of a cold-sensitive microsomal enzyme. J Biol Chem. 1973 Jul 10;248(13):4731–4738;

21. Roitelman J, Olender EH, Bar-Nun S, Dunn WA, Jr., Simoni RD. Immunological evidence for eight spans in the membrane domain of 3-hydroxy-3-methylglutaryl coenzyme A reductase: implications for enzyme degradation in the endoplasmic reticulum. J. Cell Biol. 1992;117:959–973;

22. Liscum L, Finer-Moore J, Stroud RM, Luskey KL, Brown MS, Goldstein JL. Domain structure of 3-hydroxy-3-methylglutaryl coenzyme A reductase, a glycoprotein of the endoplasmic reticulum. J Biol Chem. 1985 Jan 10;260(1):522–530;

23. Istvan ES, Palnitkar M, Buchanan SK, Deisenhofer J: Crystal structure of the catalytic portion of human HMG-CoA reductase: insights into regulation of activity and catalysis. *EMBO J* 2000, 19:819-830;

24. K. Frimpong, V.W. Rodwell, Catalysis by syrian hamster 3-hydroxy-3-methylglutaryl-coenzyme A reductase. Proposed roles of histidine 865, glutamate 558, and aspartate 766, J Biol Chem, 269 (1994), pp. 11478–11483;

25. L. Tabernero, D.A. Bochar, V.W. Rodwell, C.V. Stauffacher, Substrate-induced closure of the flap domain in the ternary complex structures provides insights into the mechanism of catalysis by 3-hydroxy-3-methylglutaryl-CoA reductase, Proc Natl Acad Sci USA, 96 (1999), pp. 7167–7171;

26. E.S. Istvan, J. Deisenhofer, Structural mechanism for statin inhibition of HMG-CoA reductase, Science, 292 (2001), pp. 1160–1164;

27. Brown MS, Goldstein JL. Multivalent feedback regulation of HMG CoA reductase, a control mechanism coordinating isoprenoid synthesis and cell growth. J. Lipid Res. 1980;21:505–517;

28. E.S. Istvan Bacterial and mammalian HMG-CoA reductases: related enzymes with distinct architectures Curr Opin Struct Biol, 11 (2001), pp. 746–751;

29. E.S. Istvan, J. Deisenhofer, The structure of the catalytic portion of human HMG-CoA reductase, Biochim Biophys Acta, 1529 (2000), pp. 9–18;

30. Luskey KL, Stevens B. Human 3-hydroxy-3-methylglutaryl coenzyme A reductase. Conserved domains responsible for catalytic activity and sterol-regulated degradation. J. Biol. Chem. 1985;260:10271–10277;

31. J.L. Goldstein, R.A. DeBose-Boyd, M.S. Brown, Protein sensors for membrane sterols, Cell, 124 (2006), pp. 35–46;

32. A. Radhakrishnan, Y. Ikeda, H.J. Kwon, M.S. Brown, J.L. Goldstein, Sterol-regulated transport of SREBPs from endoplasmic reticulum to Golgi: oxysterols block transport by binding to Insig, Proc Natl Acad Sci USA, 104 (2007), pp. 6511–6518;

33. K. Frimpong, V.W. Rodwell, The active site of hamster 3-hydroxy-3-methylglutaryl-CoA reductase resides at the subunit interface and incorporates catalytically essential acidic residues from separate polypeptides, J Biol Chem, 269 (1994), pp. 1217–1221;

34. Gil G, Faust JR, Chin DJ, Goldstein JL, Brown MS. Membrane-bound domain of HMG CoA reductase is required for sterol-enhanced degradation of the enzyme. Cell. 1985;41:249–258;

35. P.R. Clarke, D.G. Hardie, Regulation of HMG-CoA reductase: identification of the site phosphorylated by the AMP-activated protein kinase in vitro and in intact rat liver. EMBO J, 9 (1990), pp. 2439–2446;

36. D.G. Hardie, S.A. Hawley, J.W. Scott, AMP-activated protein kinase – development of the energy sensor concept, J Physiol, 574 (2006), pp. 7–15;

37. J.A. Friesen, V.W. Rodwell, The 3-hydroxy-3-methylglutaryl coenzyme-A (HMG-CoA) reductases, Genome biol, 5 (2004), p. 248;

38. P.Y. Lum, S. Edwards, R. Wright, Molecular, functional and evolutionary characterization of the gene encoding HMG-CoA reductase in the fission yeast, *Schizosaccharomyces pombe*, Yeast, 12 (1996), pp. 1107–1124;

39. J.S. Burg, D.W. Powell, R. Chai, A.L. Hughes, A.J. Link, P.J. Espenshade, Insig regulates HMG-CoA reductase by controlling enzyme phosphorylation in fission yeast, Cell Metab, 8 (2008), pp. 522–531;

40. Rudolf Schoenheimer and, Fritz Breusch, Synthesis and destruction of cholesterol in the organism *J. Biol. Chem. 1933 103: 439-448;*

41. M.D. Siperstein, M.J. Guest, Studies on the site of the feedback control of cholesterol synthesis, J Clin Invest, 39 (1960), pp. 642–652;

42. Brown, M. S., S. E. Dana, and J. L. Goldstein.Regulation of 3-hydroxy-3-methylglutaryl coenzyme A reductase activity in human fibroblasts by lipoproteins. Proc. Natl. Acad. Sci. USA1973. 70: 2 162-2 166;

43. Brown, M. S., and J. L. Goldstein. Receptor-mediated endocytosis: insights from the lipoprotein receptor system. Proc. Natl. Acad. Sci. USA. 1979.76: 3330-3337;

44. L.P. Sun, J. Seemann, J.L. Goldstein, M.S. Brown, Sterol-regulated transport of SREBPs from endoplasmic reticulum to Golgi: Insig renders sorting signal in Scap inaccessible to COPII proteins, Proc Natl Acad Sci USA, 104 (2007), pp. 6519–6526;

45. P.J. Espenshade, A.L. Hughes, Regulation of sterol synthesis in eukaryotes, Annu Rev Genet, 41 (2007), pp. 401–427;

46. Z. Kostova, Y.C. Tsai, A.M. Weissman, Ubiquitin ligases, critical mediators of endoplasmic reticulum-associated degradation, Semin Cell Dev Biol, 18 (2007), pp. 770–779;

47. V. Janssens, J. Goris, Protein phosphatase 2A: a highly regulated family of serine/threonine phosphatases implicated in cell growth and signaling, Biochem J, 353 (2001), pp. 417–439;

48. Ravid T., Doolman R., Avner R., Harats D., Roitelman J.;The Ubiquitin-Proteasome Pathway Mediates the Regulated Degradation of Mammalian 3-Hydroxy-3-methylglutaryl-coenzyme A Reductase (2000) J. Biol. Chem. 275, 35840–35847;

49. Sever N., Song B. L., Yabe D., Goldstein J. L., Brown M. S., DeBose-Boyd R. A. Insig-dependent ubiquitination and degradation of mammalian 3-hydroxy-3-methylglutaryl-CoA reductase stimulated by sterols and geranylgeraniol. J. Biol. Chem. , (2003) 278, 52479–52490;

50. B.L. Song, N. Sever, R.A. DeBose-Boyd, Gp78, a membrane-anchored ubiquitin ligase, associates with Insig-1 and couples sterol-regulated ubiquitination to degradation of HMG CoA reductase, Mol Cell, 19 (2005), pp. 829–840;

51. Bonifacino J. S., Weissman A. M Ubiquitin and the control of protein fate in the secretory and endocytic pathwaysAnnu. Rev. Cell Dev. Biol. (1998) 14, 19–57;

52. Hampton R. Y., Garza R. M. Protein quality control as a strategy for cellular regulation: lessons from ubiquitin-mediated regulation of the sterol pathway. Chem. Rev. (2009) 109, 1561–1574;

53. Leichner G. S., Avner R., Harats D., Roitelman J. Dislocation of HMG-CoA reductase and Insig-1, two polytopic endoplasmic reticulum proteins, en route to proteasomal degradation, (2009) Mol. Biol. Cell 20, 3330–3341;

54. Song B. L., DeBose-Boyd R. A. Insig-dependent Ubiquitination and Degradation of 3-Hydroxy-3-methylglutaryl Coenzyme A Reductase Stimulated by {delta}- and {gamma}-Tocotrienols (2006) J. Biol. Chem. 281, 25054–25061;

55. Roitelman J., Masson D., Avner R., Ammon-Zufferey C., Perez A., Guyon-Gellin Y., Bentzen C. L., Niesor E. J. Apomine, a novel hypocholesterolemic agent, accelerates degradation of 3-hydroxy-3-methylglutaryl-coenzyme A reductase and stimulates low density lipoprotein receptor activity (2004) J. Biol. Chem. 279, 6465–6473;

56. Ravid T, Doolman R, Avner R, Harats D, Roitelman J. The ubiquitin-proteasome pathway mediates the regulated degradation of mammalian 3-hydroxy-3-methylglutaryl-coenzyme A reductase. J. Biol. Chem. 2000;275:35840–35847;

57. Andreasen AA, Stier TJB. Anaerobic nutrition of Saccharomyces cerevisiae. I. Ergosterol requirement for growth in a defined medium. J Cell Physiol. 1953; 41:23–36;

58. Nes WR, Sekula BC, Nes WD, Adler JH. The functional importance of structural features of ergosterol in yeast. J Biol Chem. 1978; 253:6218–25;

59. Lees ND, Bard M, Kirsch DR. Biochemistry and molecular biology of sterol synthesis in Saccharomyces cerevisiae. Crit Rev Biochem Mol Biol. 1999; 34:33–47;

60. R. Hampton, D. Dimster-Denk, J. Rine, The biology of HMG-CoA reductase: the pros of contra-regulation, Trends Biochem Sci, 21 (1996), pp. 140–145;

61. M.E. Basson, M. Thorsness, J. Rine, *Saccharomyces cerevisiae* contains two functional genes encoding 3-hydroxy-3-methylglutaryl-coenzyme A reductase, Proc Natl Acad Sci USA, 83 (1986), pp. 5563–5567;

62. R.Y. Hampton, J. Rine, Regulated degradation of HMG-CoA reductase, an integral membrane protein of the endoplasmic reticulum, in yeast, J Cell Biol, 125 (1994), pp. 299–312;

63. M. Thorsness, W. Schafer, L. D'Ari, J. Rine, Positive and negative transcriptional control by heme of genes encoding 3-hydroxy-3-methylglutaryl coenzyme A reductase in *Saccharomyces cerevisiae*, Mol Cell Biol, 9 (1989), pp. 5702–5712;

64. D. Dimster-Denk, M.K. Thorsness, J. Rine, Feedback regulation of 3-hydroxy-3-methylglutaryl coenzyme A reductase in *Saccharomyces cerevisiae*, Mol Biol Cell, 5 (1994), pp. 655–665;

65. R.Y. Hampton, H. Bhakta, Ubiquitin-mediated regulation of 3-hydroxy-3-methylglutaryl-CoA reductase, Proc Natl Acad Sci USA, 94 (1997), pp. 12944–12948;

66. R.Y. Hampton, R.M. Garza, Protein quality control as a strategy for cellular regulation: lessons from ubiquitin-mediated regulation of the sterol pathway, Chem Rev, 109 (2009), pp. 1561–1574;

67. Endo, A., M. Kuroda, and K. Tanzawa. Competitive inhibition of 3-hydroxy-3-methylglutaryl coenzyme A reductase by ML-236A and ML-236B fungal metabolites, having hypocholesterolemic activity. FEBS Lett. 1976.72: 323-326;

68. Brown,M. S., J. R. Faust, J. L. Goldstein, I. Kaneko, and A. Endo. Induction of 3-hydroxy-3-methyl-glutaryl coenzyme A reductase activity in human fibroblasts incubated with compactin (ML-236B), a competitive inhibitor of the reductase. J. Bid. Chem. 1978. 253: 1121-1128;

69. Kaneko, I., Y. Hazama-Shimada, and A. Endo. Inhibitory effects on lipid metabolism in cultured cells of ML-236B, a potent inhibitor of 3-hydroxy-3-methyl-glutaryl-coenzyme-A reductase. Eur. J. Biochem. 1978. 87:313-321;

70. Hamilton-Craig I. Statin-associated myopathy. Med J Aust 2001; 175: 486-489;

71. Rozman D, Monostory K. Perspectives of the non-statin hypolipidemic agents. Pharmacol Ther 2010; 127: 19-40;

72. Cham S, Evans MA, Denenberg JO, Golomb BA. Statin associated muscle-related adverse effects: a case series of 354 patients. Pharmacotherapy 2010; 30: 541-553;

73. E. M. deGoma, D. J. Rader, Novel HDL-directed pharmacotherapeutic strategies, Nat Rev Cardiol 2011, 8(5), 266-277;

74. S. Gorinstein, H. Leontowicz, M. Leontowicz, R. Krzeminski, M. Gralak, O. Martin-Belloso, E. Delgado-Licon, R. Haruenkit, E. Katrich, Y. S. Park, S. T. Jung, S.Trakhtenberg, Fresh israeli jaffa blond (Shamouti) orange and israeli jaffa red starruby (sunrise) grapefruit juices affect plasma lipid metabolism and antioxidant capacity in rats fed added cholesterol J Agric Food Chem 2004, 52(15), 4853-4859;

75. M. T. Monforte, A. Trovato, S. Kirjavainen, A. M. Forestieri, E. M. Galati, R. B. Lo Curto, Biological effects of hesperidin, a citrus flavonoid. Note 2: Hypolipidemic activity on experimental hypercholesterolemia in rat, Farmaco 1995, 50(9), 595-599;

76. S. Gorinstein, H. Leontowicz, M. Leontowicz, R. Krzeminski, M. Gralak, E. Delgado-Licon, A. L. Martinez Ayala, E. Katrich, S. Trakhtenberg, hanges in plasma lipid and antioxidant activity in rats as a result of naringin and red grapefruit supplementation J Agric Food Chem 2005, 53(8), 3223-3228;

77. D. Barreca, E. Bellocco, C. Caristi, U. Leuzzi, G. Gattuso, Flavonoid composition and antioxidant activity of juices from chinotto (*Citrus x myrtifolia* Raf.) fruits at different ripening stages J Agric Food Chem 2007, 58(5), 3031-3036;

78. G. Gattuso, C. Caristi, C. Gargiulli, E. Bellocco, G. Toscano, U. Leuzzi, Flavonoid Glycosides in Bergamot Juice (Citrus bergamia Risso) J Agric Food Chem 2006, 54(11), 3929-3935;

79. P. Dugo, M. L. Presti, M. Ohman, A. Fazio, G. Dugo, L. Mondello, Determination of flavonoids in citrus juices by micro-HPLC-ESI/MS, J Sep Sci 2005, 28(11), 1149-1156;

80. Nogata, K. Sakamoto, H. Shiratsuchi, T. Ishii, M. Yano, H. Ohta, Flavonoid composition of fruit tissues of citrus species Biosci Biotechnol Biochem 2006, 70(1), 178-192;

81. L. Di Donna, G. De Luca, F. Mazzotti, A. Napoli, R. Salerno, D. Taverna, G. Sindona, Statin-like Principles of Bergamot Fruit (*Citrus bergamia*): Isolation of 3-Hydroxymethylglutaryl Flavonoid Glycosides, J Nat Prod 2009, 72(7), 1352-1354;

82. N. Miceli, M. R. Mondello, M. T. Monforte, V. Sdrafkakis, P. Dugo, M. L. Crupi,M. F. Taviano, R. De Pasquale, A. Trovato, Hypolipidemic effects of Citrus bergamia Risso et Poiteau juice in rats fed a hypercholesterolemic diet. J Agric Food Chem 2007, 55(26), 10671-10677;

83. Rai SK, Sharma M, Tiwari M., Inhibitory effect of novel diallyldisulfide analogs on HMG-CoA reductase expression in hypercholesterolemic rats: CREB as a potential upstream target. Life Sci. 2009 Jul 31;85(5-6):211-9;

84. M. R. Muci, A. R. Cappello, G. Vonghia, E. Bellitti, L. Zezza, G. V. Gnoni, Change in cholesterol levels and in lipid fatty acid composition in safflower oil fed lambs Int JVitam Nutr Res 1992, 62(4), 330-333;

85. E. G. Bligh, W. J. Dyer, Can A rapid method for total lipid extraction and purification J Biochem Physiol 1959, 37(8), 911-917;

86. V. Dolce, P. Scarcia, D. Iacopetta, F. Palmieri, A fourth ADP/ATP carrier isoform in man: identification, bacterial expression, functional characterization and tissue distribution FEBS Lett 2005, 579(3), 633-637;

87. A. Caputi Jambrenghi, G. Paglialonga, A. Gnoni, F. Zanotti, F. Giannico, G. Vonghia, G. V. Gnoni, Changes in lipid composition and lipogenic enzyme activities in liver of lambs fed omega-6 polyunsaturated fatty acids. Comp Biochem Physiol B Biochem Mol Biol 2007, 147(3), 498-503;

88. Folch J, Lees M, Sloane Stanley Gh. A simple method for the isolation and purification of total lipides from animal tissues. J Biol Chem. 1957 May;226(1):497-509;

89. I. W. Duncan, P. H. Culbreth, C. A. Burtis, Determination of free, total, and esterified cholesterol by high-performance liquid chromatography J Chromatogr 1979, 162(3), 281-292;

90. Carrisi C, Madeo M, Morciano P, Dolce V, Cenci G, Cappello AR, Mazzeo G, Iacopetta D, Capobianco L., Identification of the Drosophila melanogaster mitochondrial citrate carrier: bacterial expression, reconstitution, functional characterization and developmental distribution. J Biochem. 2008 Sep;144(3):389-92;

91. Fiermonte, G., Palmieri, L., Dolce, V., Lasorsa, F. M., Palmieri, F., Runswick, M. J. and Walker, J. E. Identification of the human mitochondrial oxodicarboxylate carrier. Bacterial expression, reconstitution, functional characterization, tissue distribution, and chromosomal location (1998) J. Biol. Chem. *273*, 24754±24759;

92. Leszczynska A, Burzynska B, Plochocka D, Kaminska J, Zimnicka M, Kania M, Kiliszek M, Wysocka-Kapcinska M, Danikiewicz W, Szkopinska A, Investigating the effects of statins on cellular lipid metabolism using a yeast expression system.. PLoS One. 2009 Dec 30;4(12):e8499;

93. Basson ME, Thorsness M, Finer-Moore J, Stroud RM, Rine J., Structural and functional conservation between yeast and human 3-hydroxy-3-methylglutaryl coenzyme A reductases, the rate-limiting enzyme of sterol biosynthesis. Mol Cell Biol. 1988 Sep;8(9):3797-808;

94. Kleinsek D A, Porter J W. An alternate method of purification and properties of rat liver β-hydroxy-β-methylglutaryl coenzyme A reductase. J Biol Chem. 1979;254:7591–7599

95. M. Madeo, C. Carrisi, D. Iacopetta, L. Capobianco, A. R. Cappello, C. Bucci, F. Palmieri, G. Mazzeo, A. Montalto, V. Dolce, Abundant expression and purification of biologically active mitochondrial citrate carrier in baculovirus-infected insect cells.J Bioenerg Biomembr 2009, 41(3), 289-297;

96. Lijnen P, Celis H, Desager JP, Fagard R. Changes in plasma lipids, lipoproteins and apolipoproteins in hypercholesterolaemic patients treated with pravastatin. J Hum Hypertens (1995) 9: 557–564;

97. Mosley ST, Kalinowski SS, Schafer BL, Tanaka RD. Tissue-selective acute effects of inhibitors of 3-hydroxy-3-metbylglutaryl coenzyme A reductase on cholesterol biosynthesis in lens. J Lipid Res. 1989;30:1411-1420;

98. Yanagita T, Yamamoto K, Ishida S, Sonda K, Morito F. Effects of simvastatin, a cholesterol synthesis inhibitor, on phosphatidylcholine synthesis in HepG2 cells. Clin Ther (1994) 16: 200–208

99. Gerber R, Ryan JD, Clark DS. Cell-based screen of HMG-CoA reductase inhibitors and expression regulators using LC-MS. Anal Biochem (2004) 329: 28–34;

ABBREVIATION INDEX

ACAT	Acyl-CoA: Cholesterol acyltransferase
AMPK	AMP-activated protein kinase
ATP	Adenosine triphosphate
BSA	Bovine serum albumin
cAMP	Cyclic adenosine monophosphate
DTE	Dithioerythritol
EDTA	Ethylenediaminetetraacetic acid
HDL	Hight density lipoprotein
HMG-CoA	3-hydroxy-3-methyl-glutaryl-CoA
HMGR	3-hydroxy-3-methyl-glutaryl-CoA reductase
IDL	Intermediate density lipoprotein
LCAT	Lecithin-cholesterol acyltransferase
IPTG	Isopropyl β-D-1-thiogalactopyranoside
LDL	Low density lipoprotein
$NADP^+$	nicotinamide adenine dinucleotide phosphate
NADPH	nicotinamide adenine dinucleotide phosphate
PMSF	phenylmethanesulfonylfluoride
RE	endoplasmic reticulum
SCAP	SREBP cleavage-activating protein
SDS	Sodium dodecyl sulfate
SREBP	Sterol regulatory element binding proteins
SSD	Sterol sensing domain
VLDL	Very low density lipoprotein